Pavia October 25, 2004

Review of Semiconductor Drift Detectors

Talk given by Pavel Rehak following a presentation on 5th Hiroshima Symposium of Semiconductor Tracking Detectors

Outline of the Review

- Principles of Semiconductor Drift Detectors
- Drift Detectors for Position and Charge sensing
- Lessons learned from utilization of Drift Detectors in Heavy Ion Experiments
- X-ray spectroscopy with Drift Detectors
- Controlled Drift Detectors
- Conclusions and predictions

Concept of Semiconductor Drift Detector

Transport of charged carriers in thin fully depleted semiconductor detectors in direction parallel to the large surface of the detector.

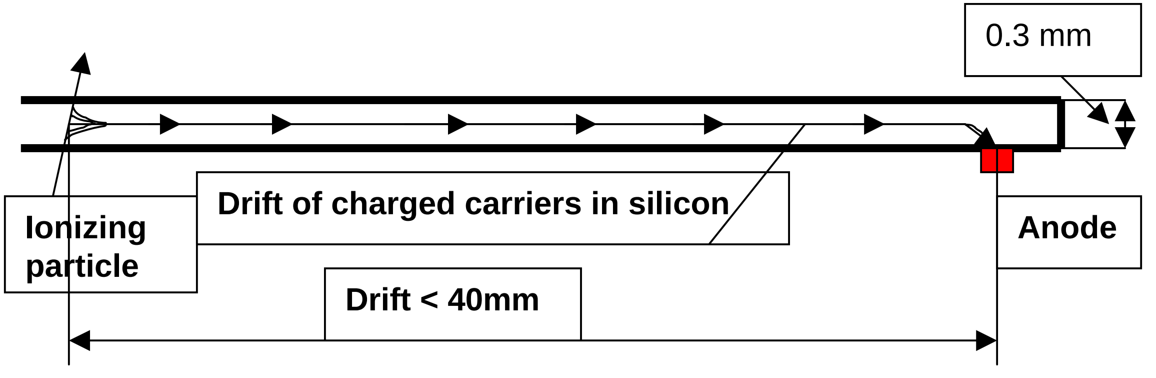

1.) Charge carriers induce a signal on the anode only on the arrival. The drift time measure the distance between the position of the ionizing particle and the anode.

2.) The capacitance of the anode is small -> low series noise of the read-out.

Analyses of buried channel Charge Coupled Devices. (CCDs) in 1983

Negative potential in the region of the channel.

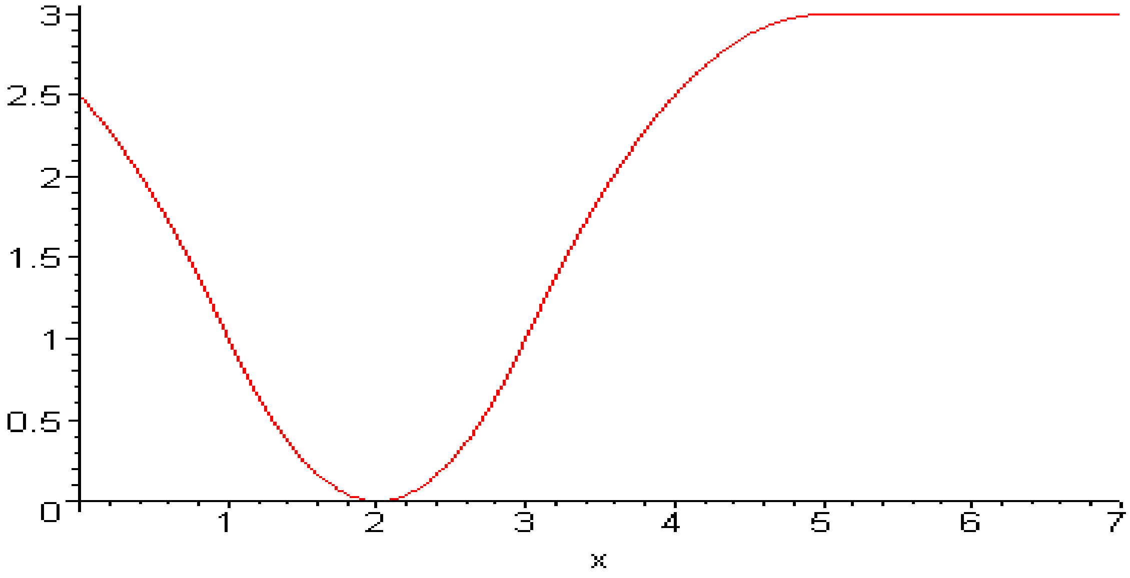

Reversed biased one sided step p-n junction in 1dimension

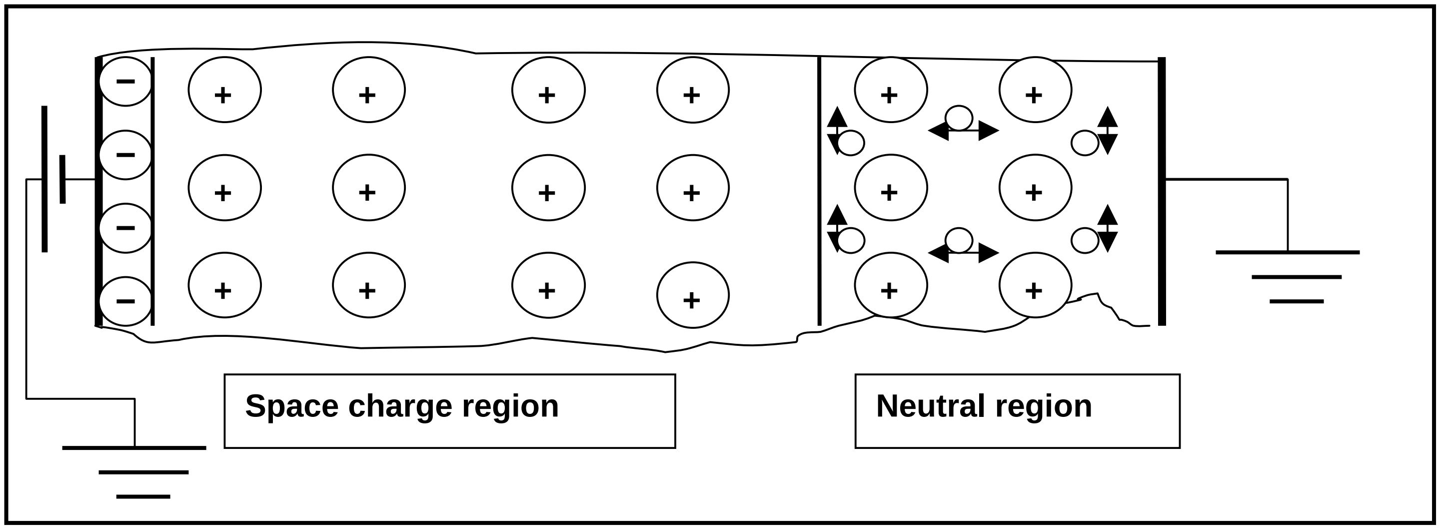

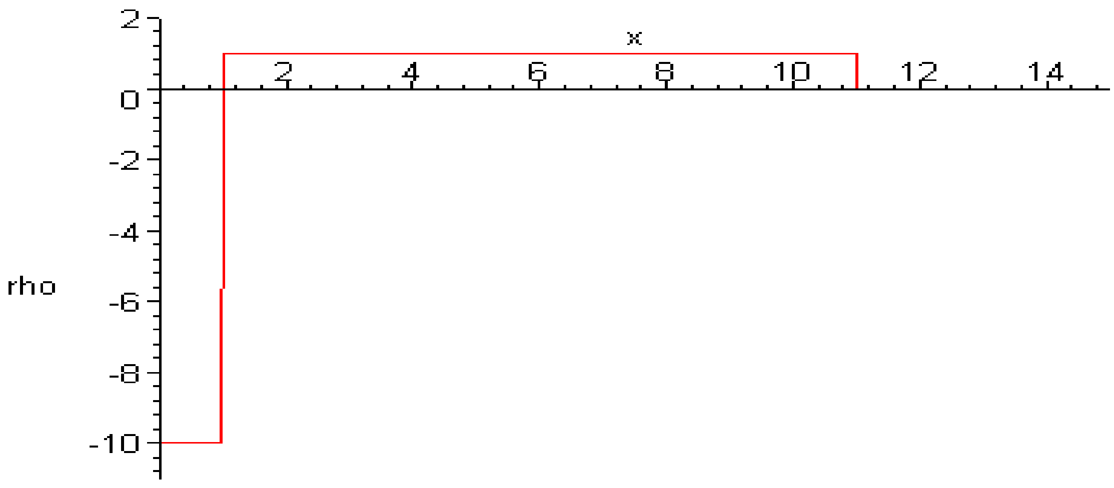

Space charge density ρ

$\rho = qN$

N is donor or acceptor volume density

Equations of electrostatics

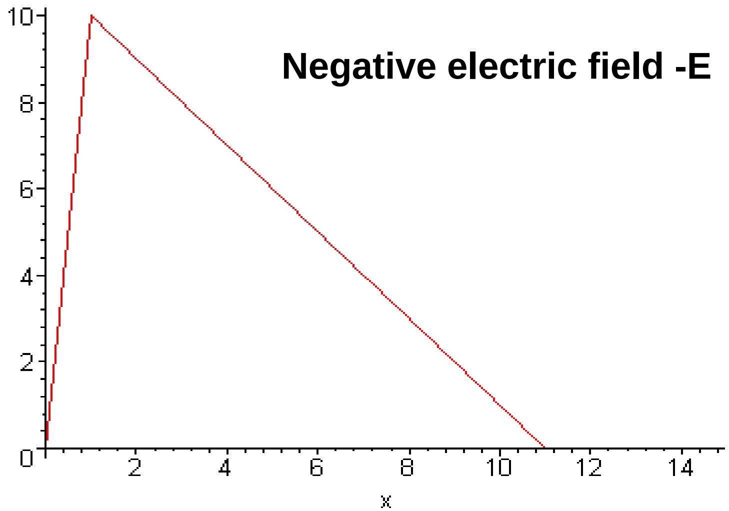

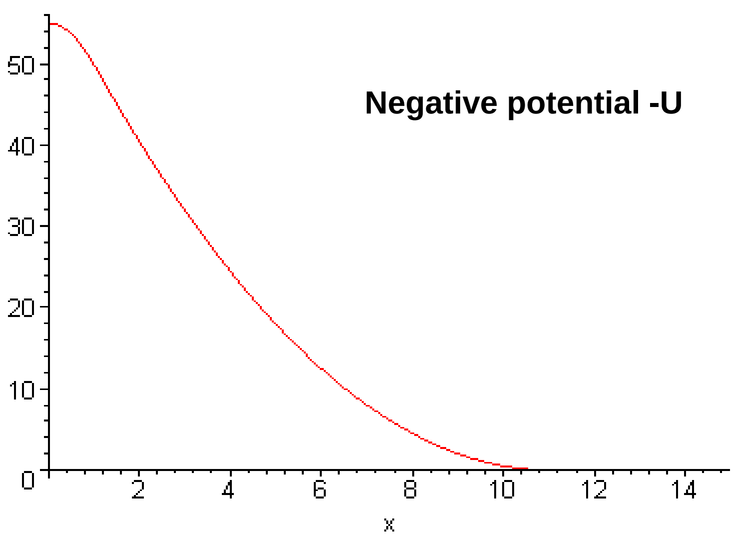

div E= ρ/ε

In one dimensional case the above reduces into: ***dE/dx=*** ρ/ε

Electric field is a piecewise linear .

Electric potential *U* is defined by:

E=-grad U

In one dimensional case the above reduces into: ***E=-dU/dx***

U is parabolic and depleted depth *d*

$$d = \sqrt{2\varepsilon U / qN}$$

Depletion from two sides

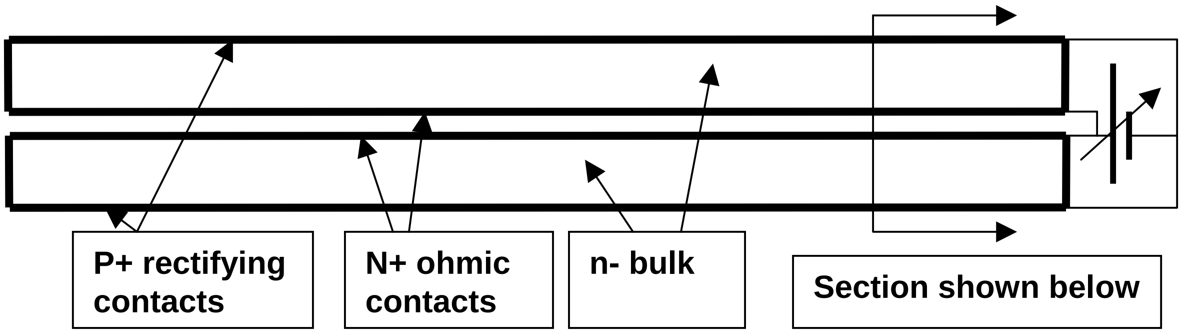

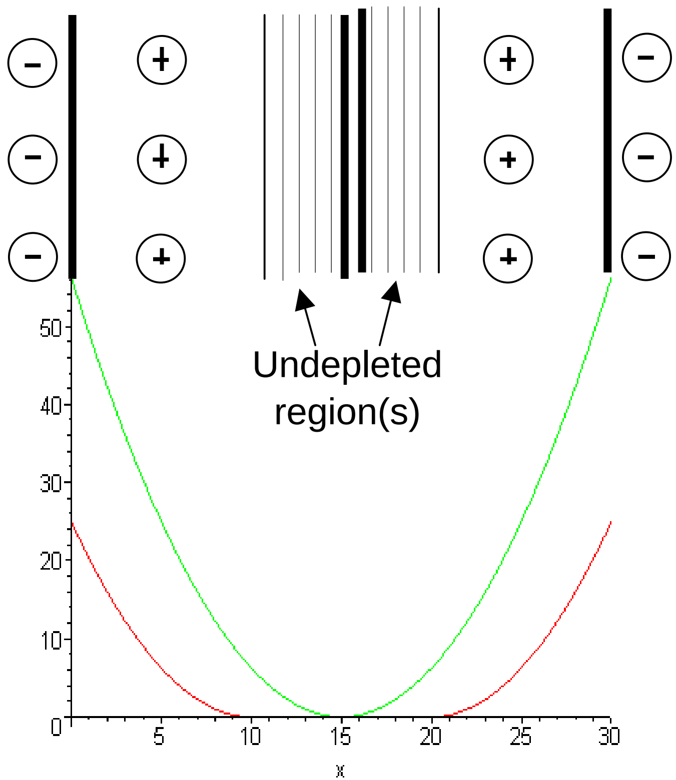

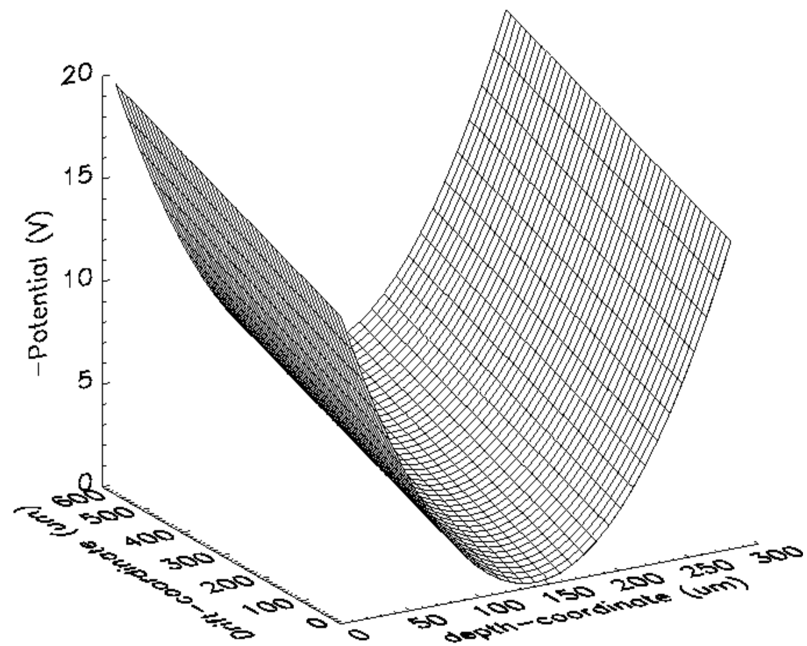

Summary of principles

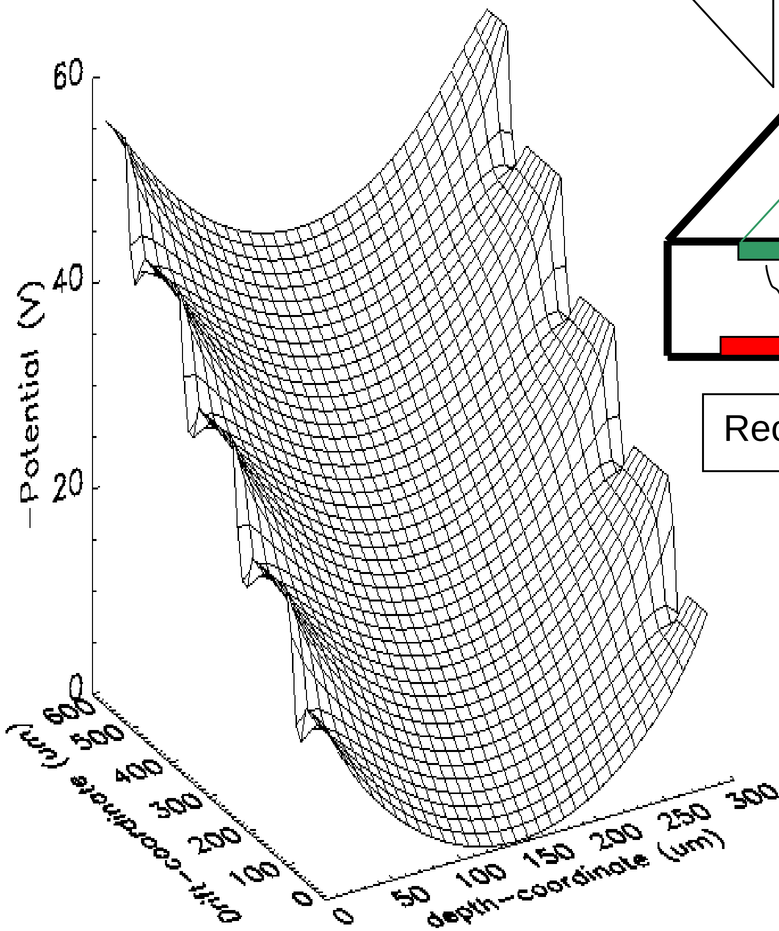

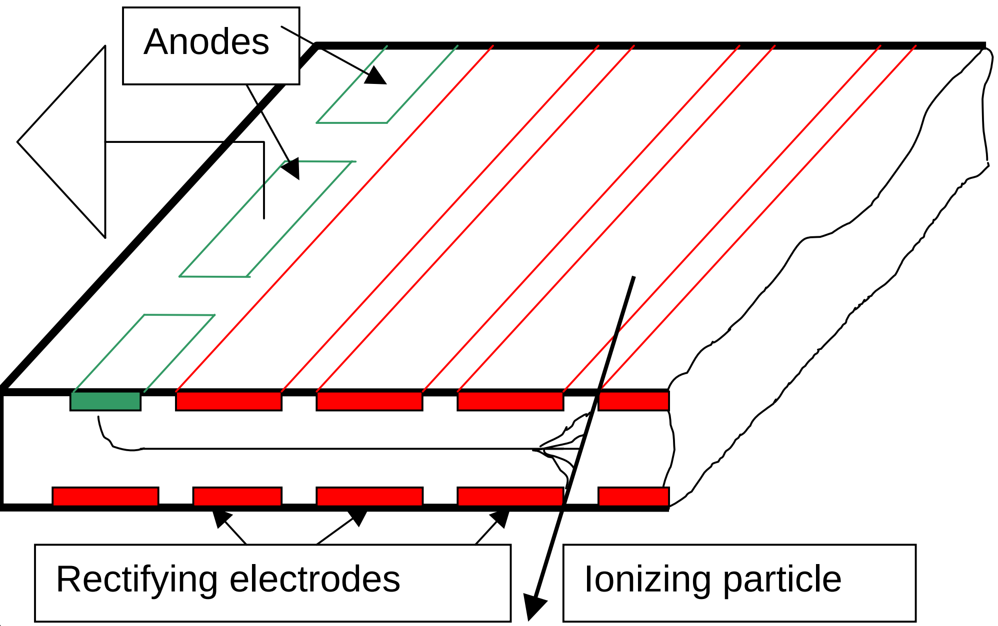

Unambiguous 2 dimensional measur.

Precision: 2um in lab

10 um in the test beam

20 um in experiments

Optimal signal processing

$$\varepsilon^2 = \frac{C^2 e_n^2 / 2\int_{-\infty}^{+\infty} w'^2(t)dt + q^2 \nu \int_{-\infty}^{+\infty} w^2(t)dt + q^2 N \int_{-\infty}^{+\infty} f(t) w^2(t)dt}{q^2 N^2 \left[\int_{-\infty}^{+\infty} f'(t) w(t) dt \right]^2}$$

Where: *w(t)* is unknown weighting function, *f(t)* is pulse shape induced on the anode normalized to the area of 1, *N* is the number of electrons in the signal pulse, *C* total input capacitance, *e_n^2* physical spectral density of the series noise, νq is the leakage current and *q* is the positive value of charge of an electron.

To minimize the above time variance can be reduced to the solution of the following equation:

$$-\frac{C^2 e_n^2}{q^2 N^2} w''(t) + \frac{2 f(t)}{N} w(t) + \frac{2\nu}{N^2} w(t) = 2\varepsilon_{\min}^2 f'(t) \cdot const$$

Position sensing in high energy heavy ion experiments

- NA45 (CERES) Experiment at SPS at CERN a) 3’’ cylindrical drift detector and b) 4’’ cylindrical detector (past)
- STAR Experiment at RHIC at BNL (present)
- ALICE Experiment at LHC at CERN (future)

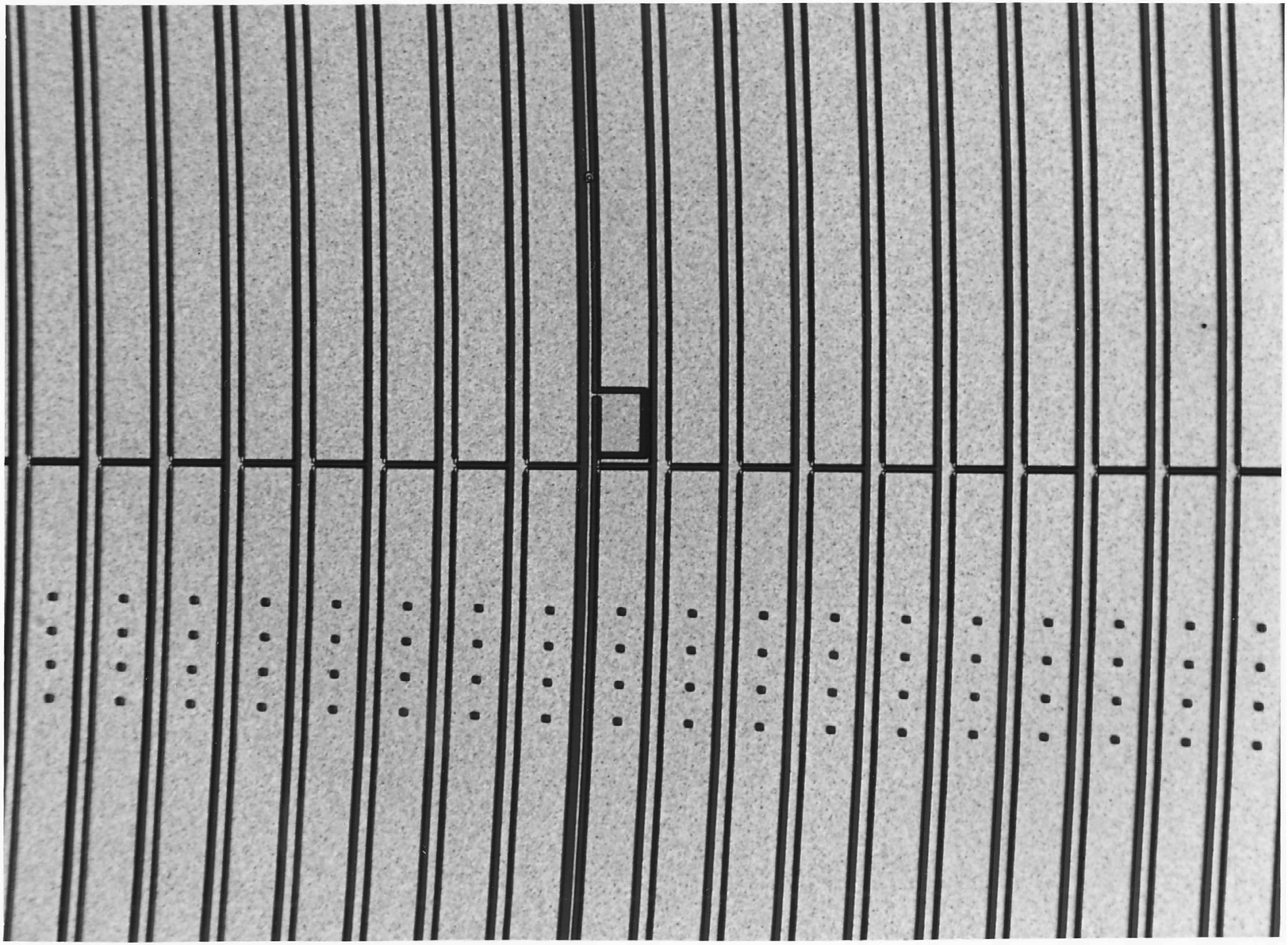

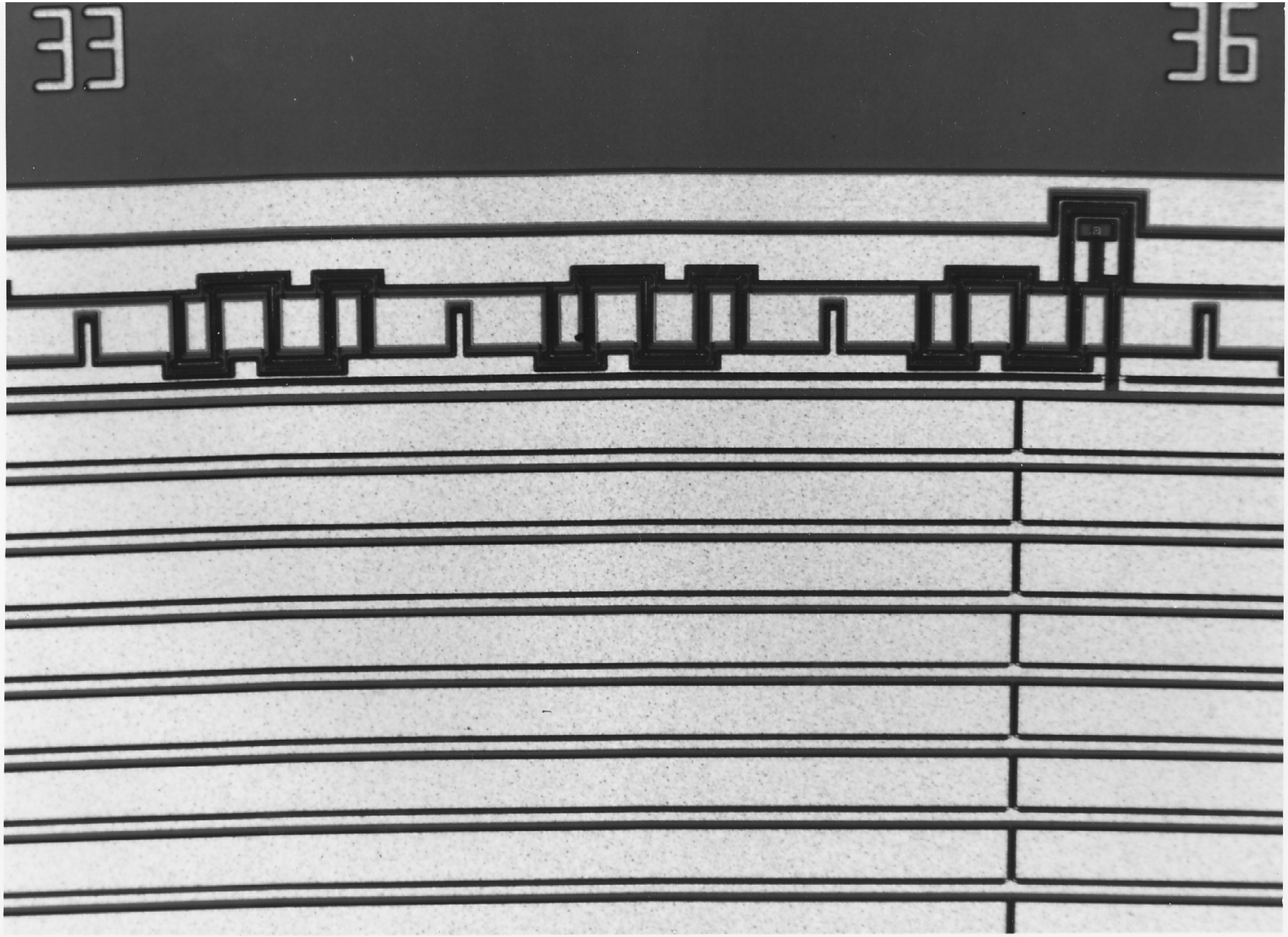
33
36

Innovations in CERES cyl. Det.

- Collection of leakage current generated at the Si-SiO interface at a sink anode
- Interlaced anodes (Nyquist filtering in linear dimension)

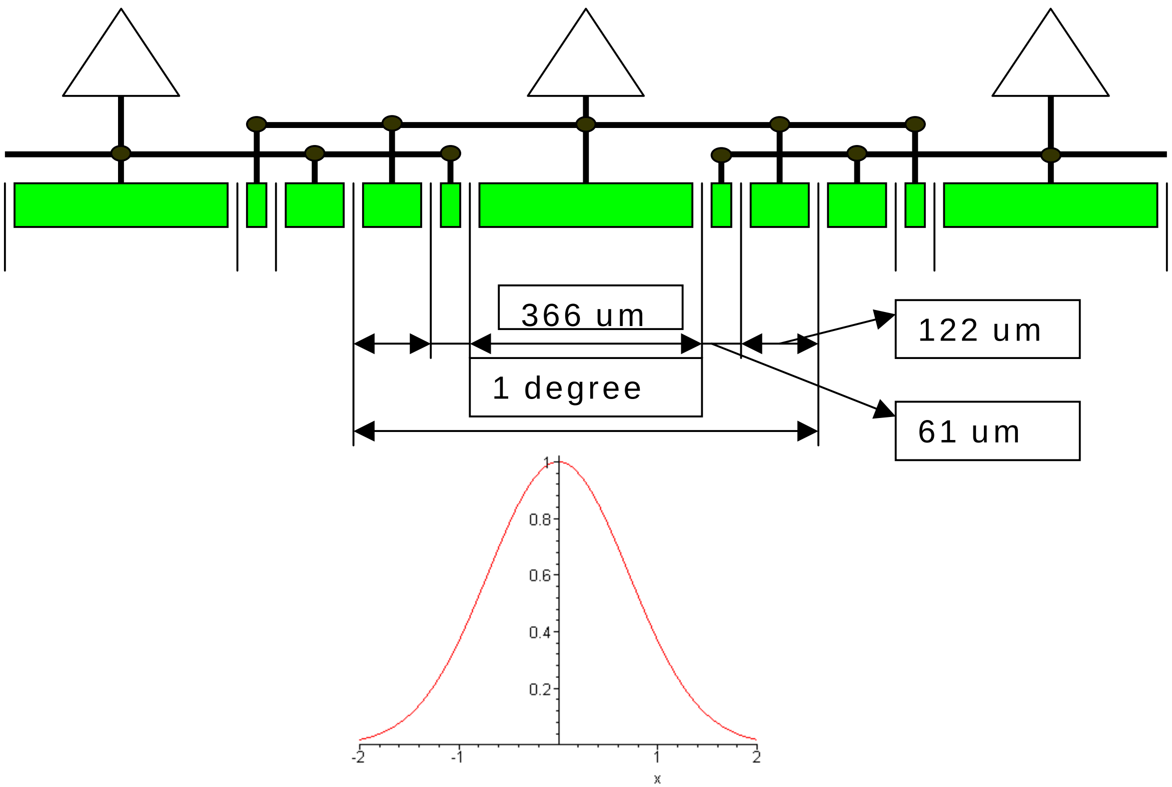

STAR Drift Detector

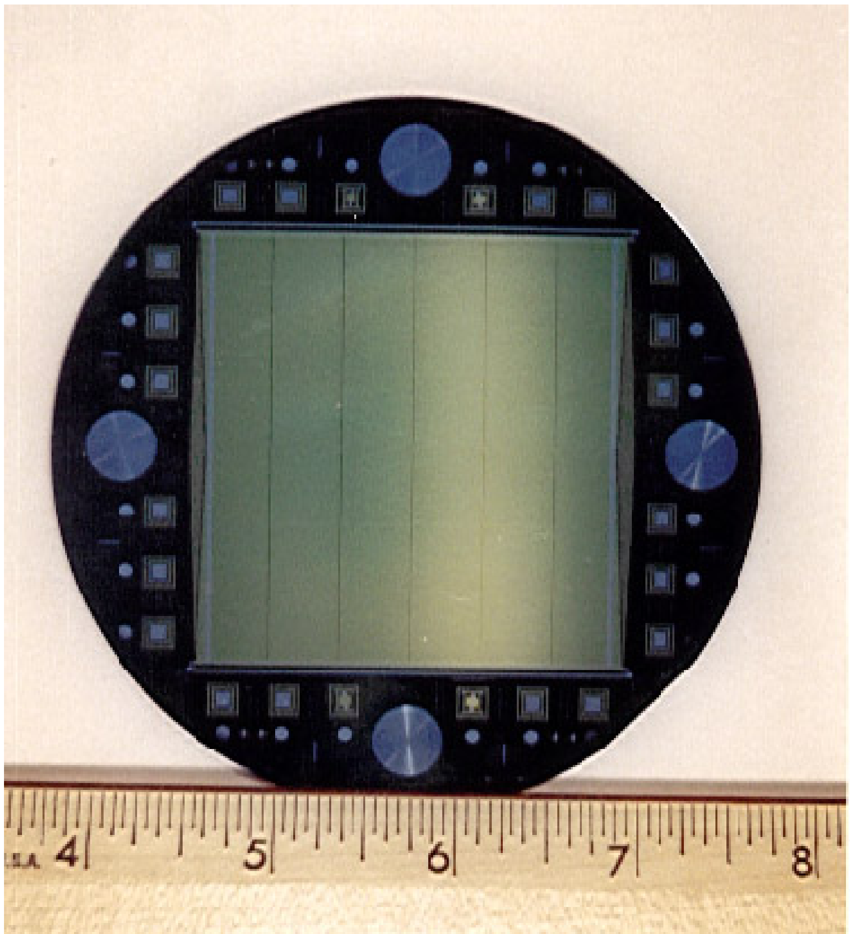

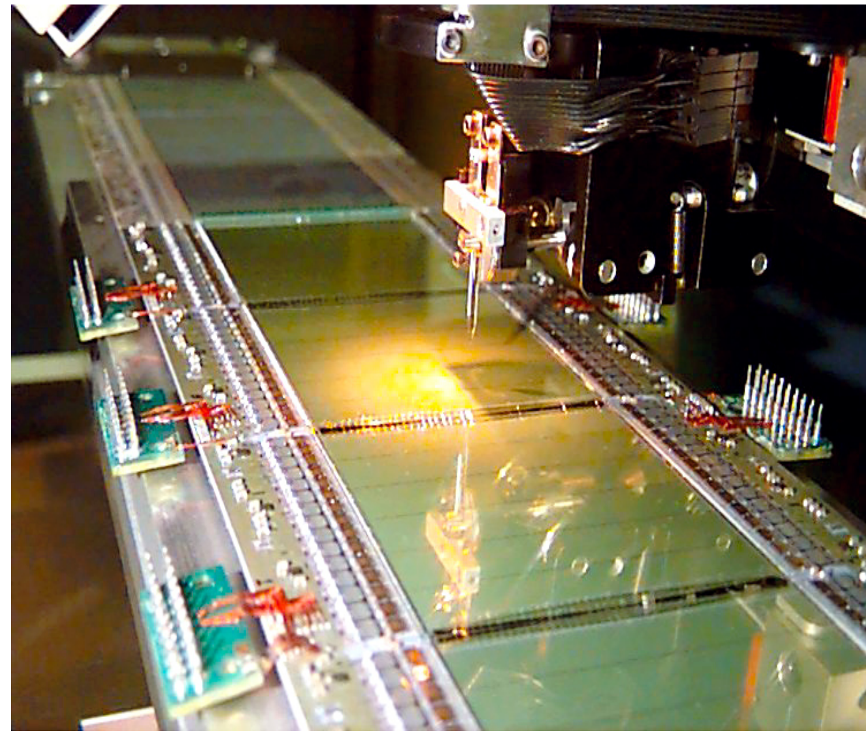

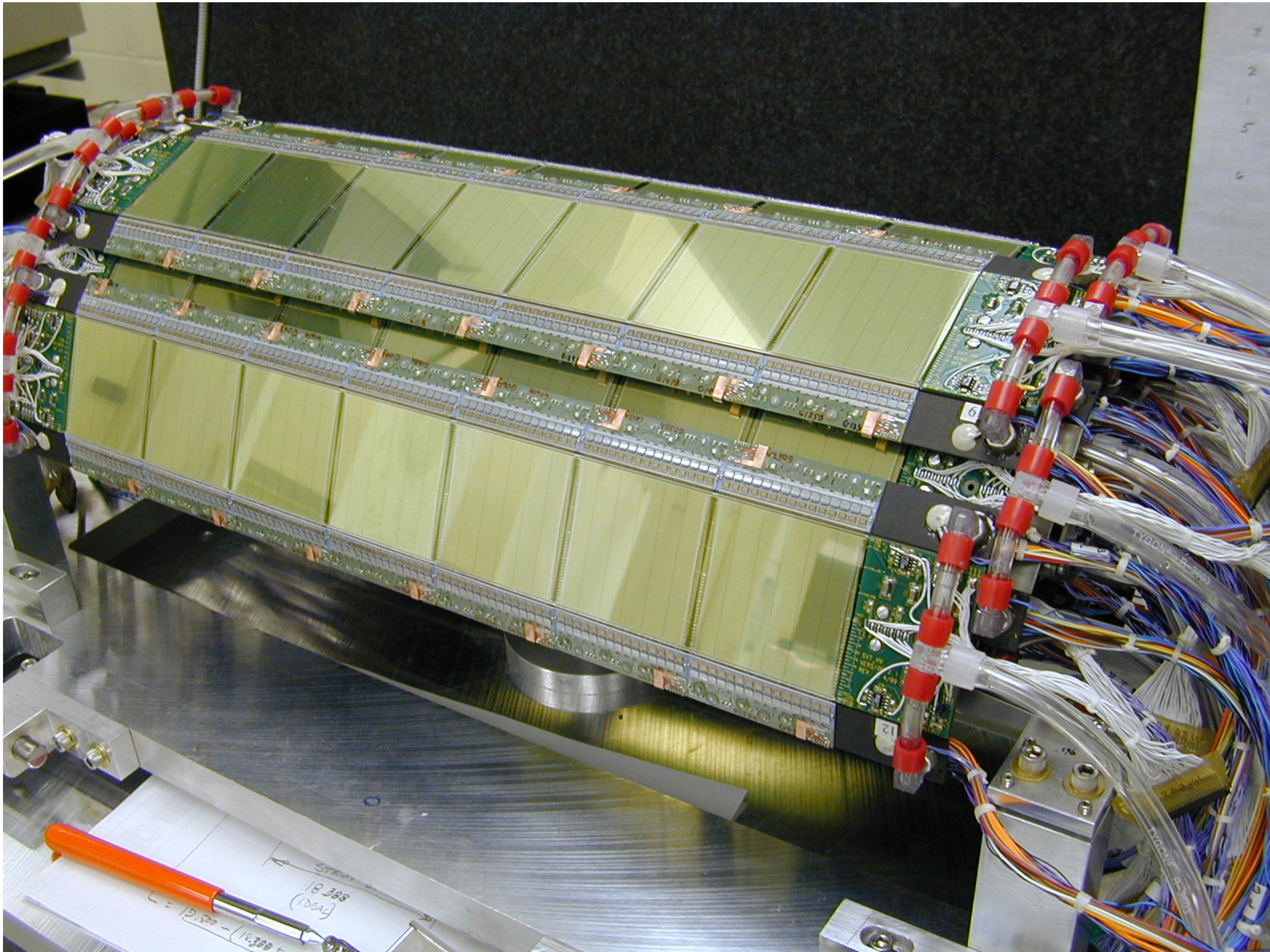

SDD collaboration

- INFN - Turin – Italy
- INFN - Trieste - Italy
- INFN - Bologna – Italy
- INFN - Rome – Italy
- INFN - Alessandria- Italy
- Ohio State University - Columbus - Ohio - USA
- University of Jyvaskyla - Jyvaskyla - Finland
- Nat. Acad. of Sciences, Bogolyubov Inst. for Th. Phys. - Kiev - Ukraine
- Scientific Res. Techn. Inst. of Instrument Making - Kharkov - Ukraine
- Acad. of Sciences of Czech Republic - Rez U Prahy - Czech Republic
- St. Petersburg State University - St. Petersburg - Russia

SDD barrels

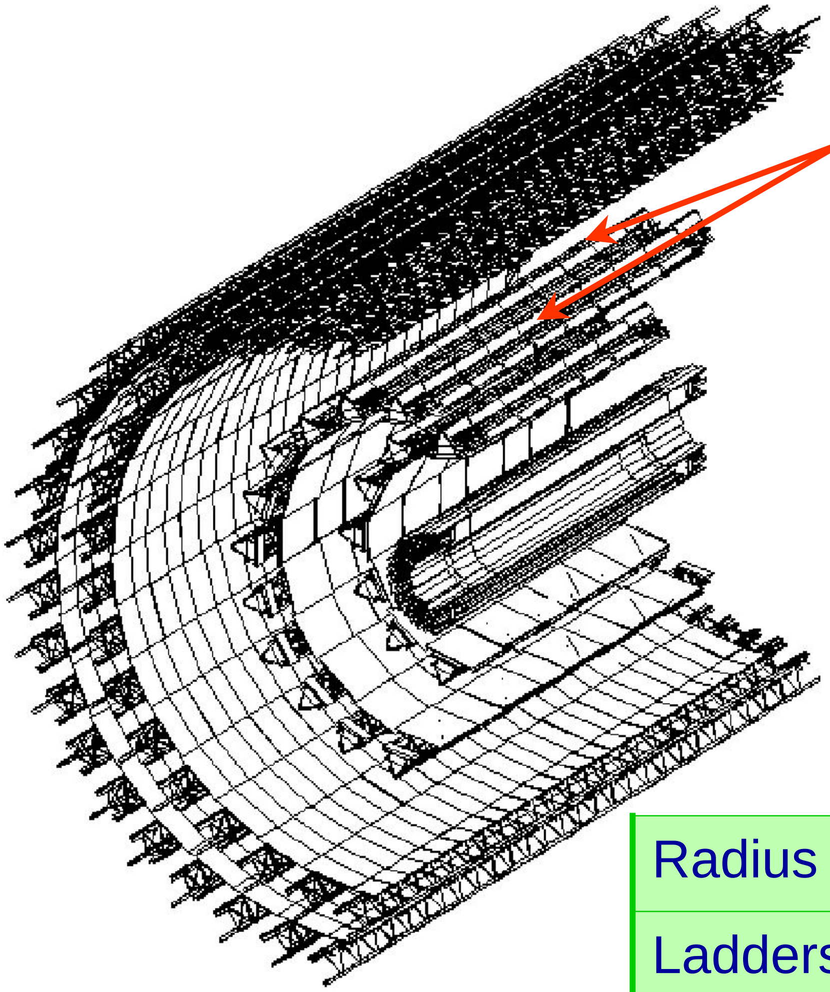

Silicon Drift Detectors

Tot. No. channels 133 •10^3

Tot. No. detectors 260

total area 1.37 m^2

	Layer 3	Layer 4
Radius (mm)	14.9	23.8
Ladders	14	22
SDDs per ladder	6	8

ALICE Silicon Drift Detector

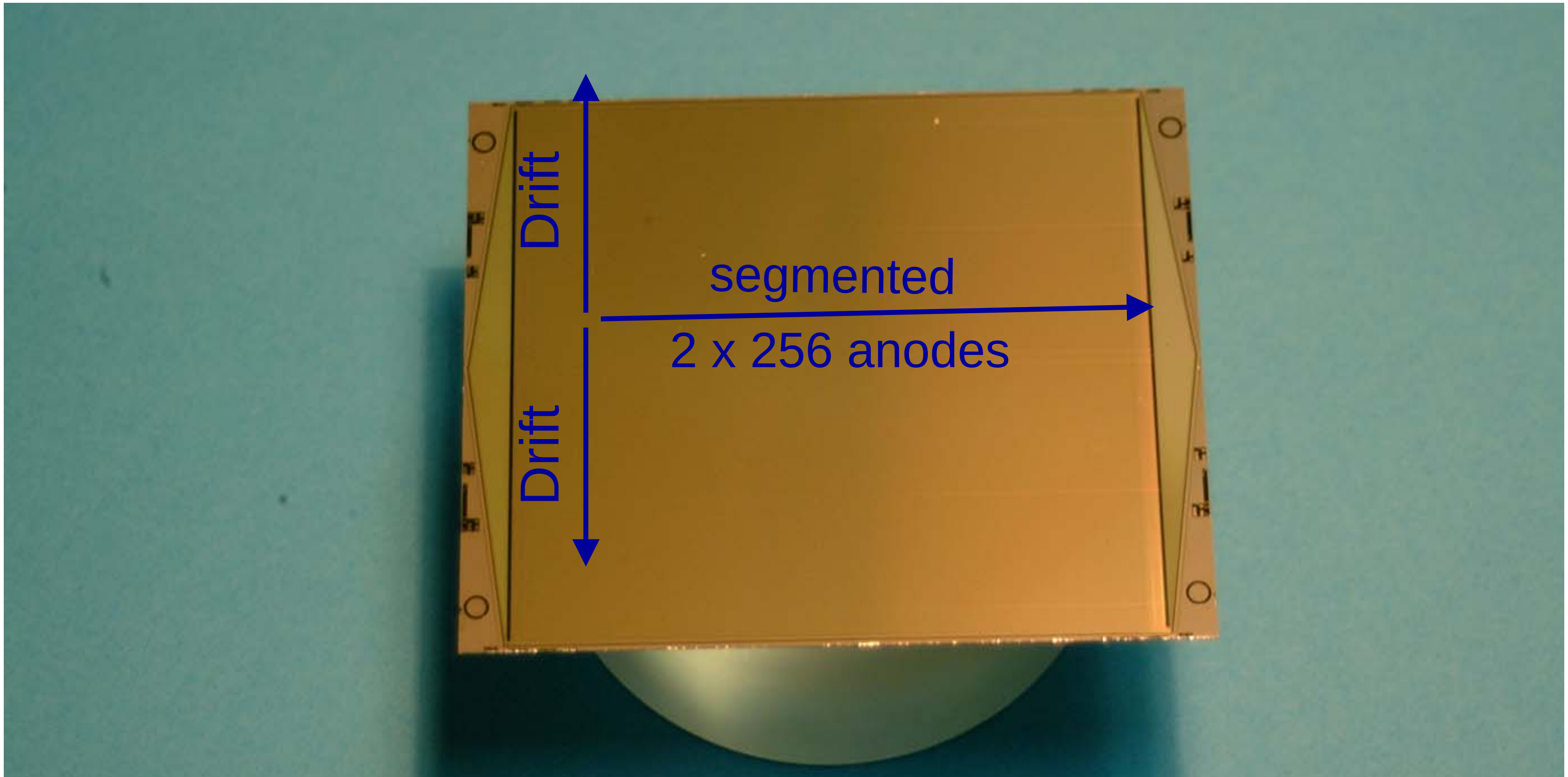

Wafer: 5”, Neutron Transmutation Doped (NTD) silicon, 3 kΩ·cm resistivity, 300 μm thickness

Active area: 7.02 × 7.53 cm^2 (83% to total)

Detector design features

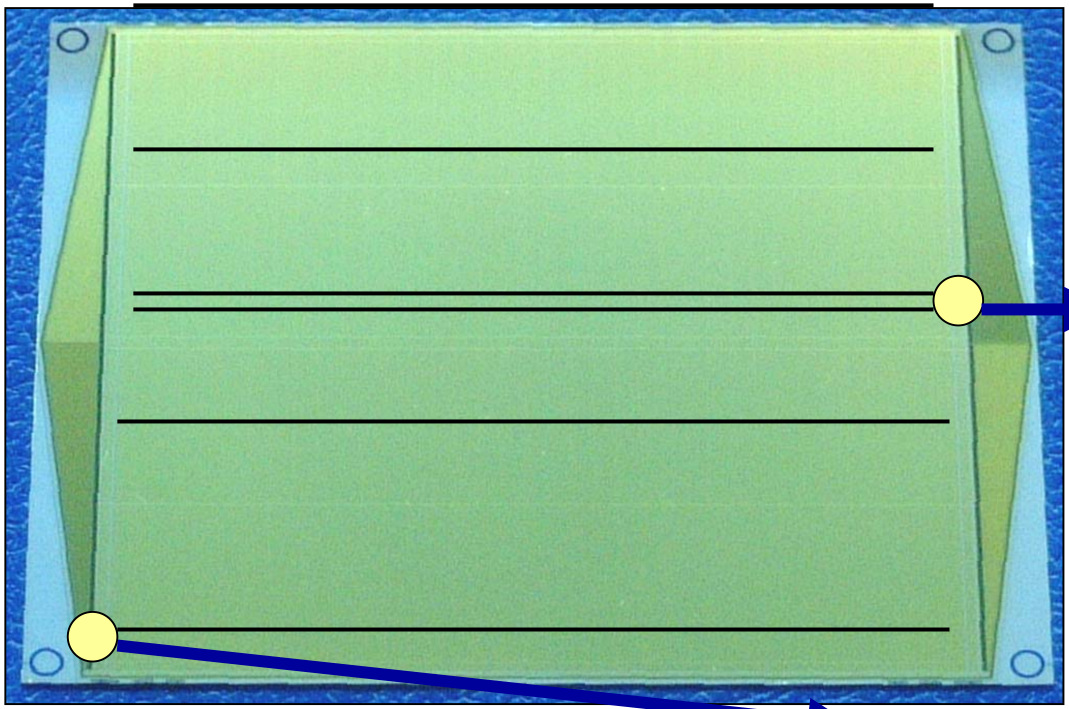

injector lines

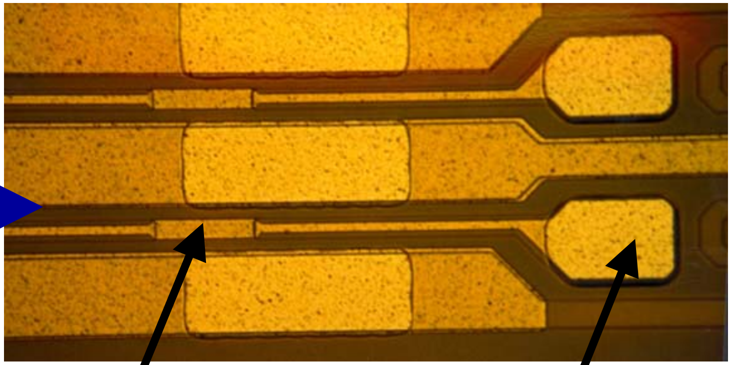

injector line bonding pad

MOS injector (every 8th anode)

Charge collection zone

guard cathodes (32 μm pitch)

292 drift cathodes (120 μm pitch)

implanted HV voltage dividers

256 collection anodes (294 μm pitch)

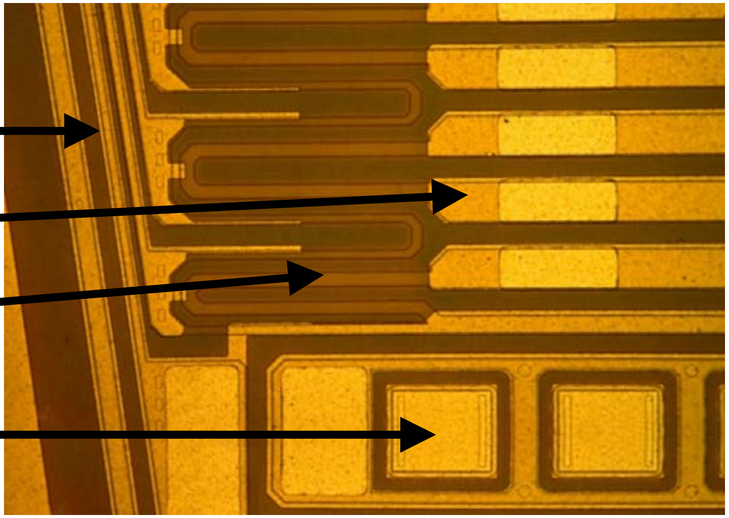

Beam Tests in 2003 – Position resolution

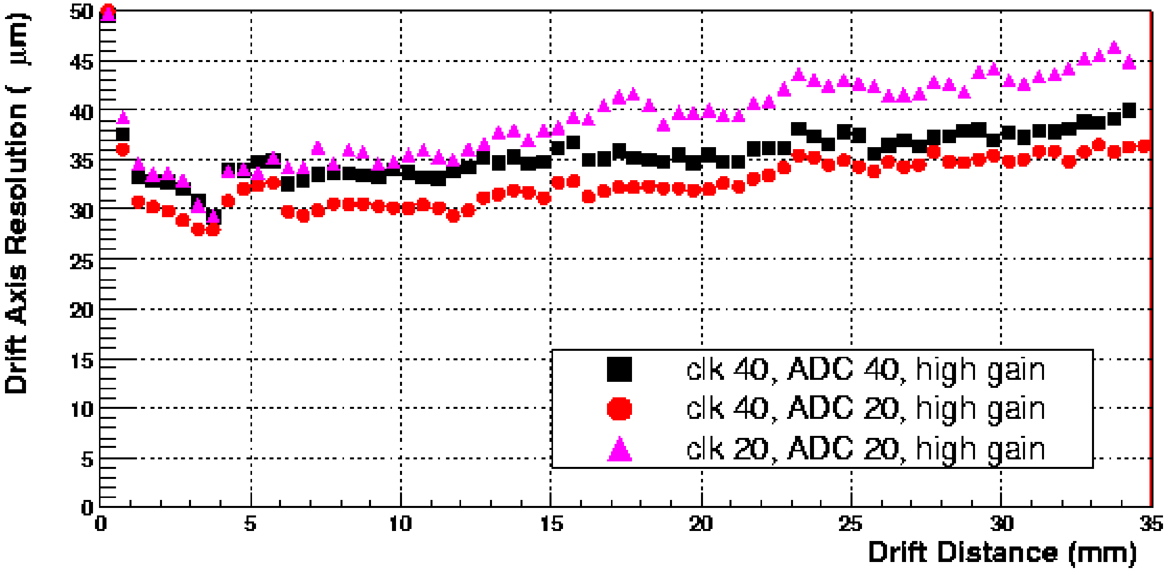

Exhaustive test of the front-end parameters performed in beam test:gain, sampling & ADC frequencies...

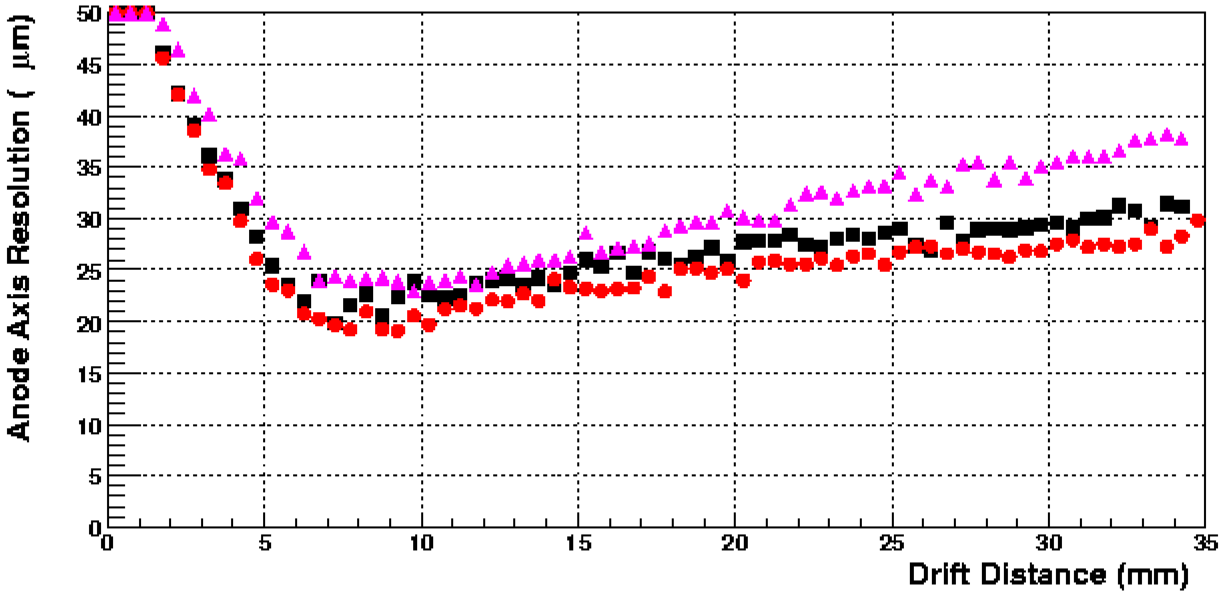

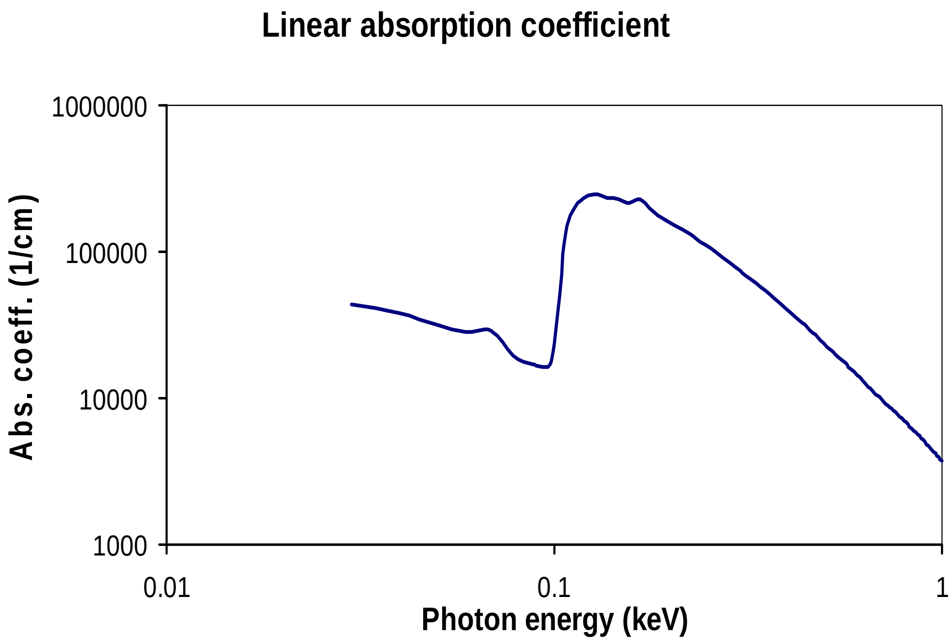

Linear absorption coefficient
Abs. coeff. (1/cm)
1000000
100000
10000
1000
0.01
0.1
1
Photon energy (keV)

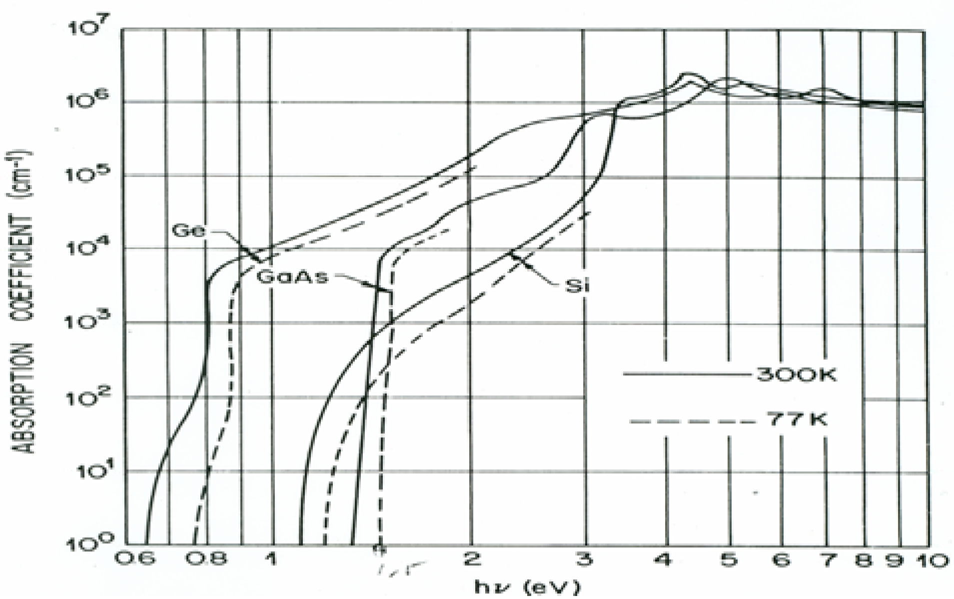

ABSORPTION COEFFICIENT (cm⁻¹)
Ge
GaAs
Si
300K
77K
hν (eV)

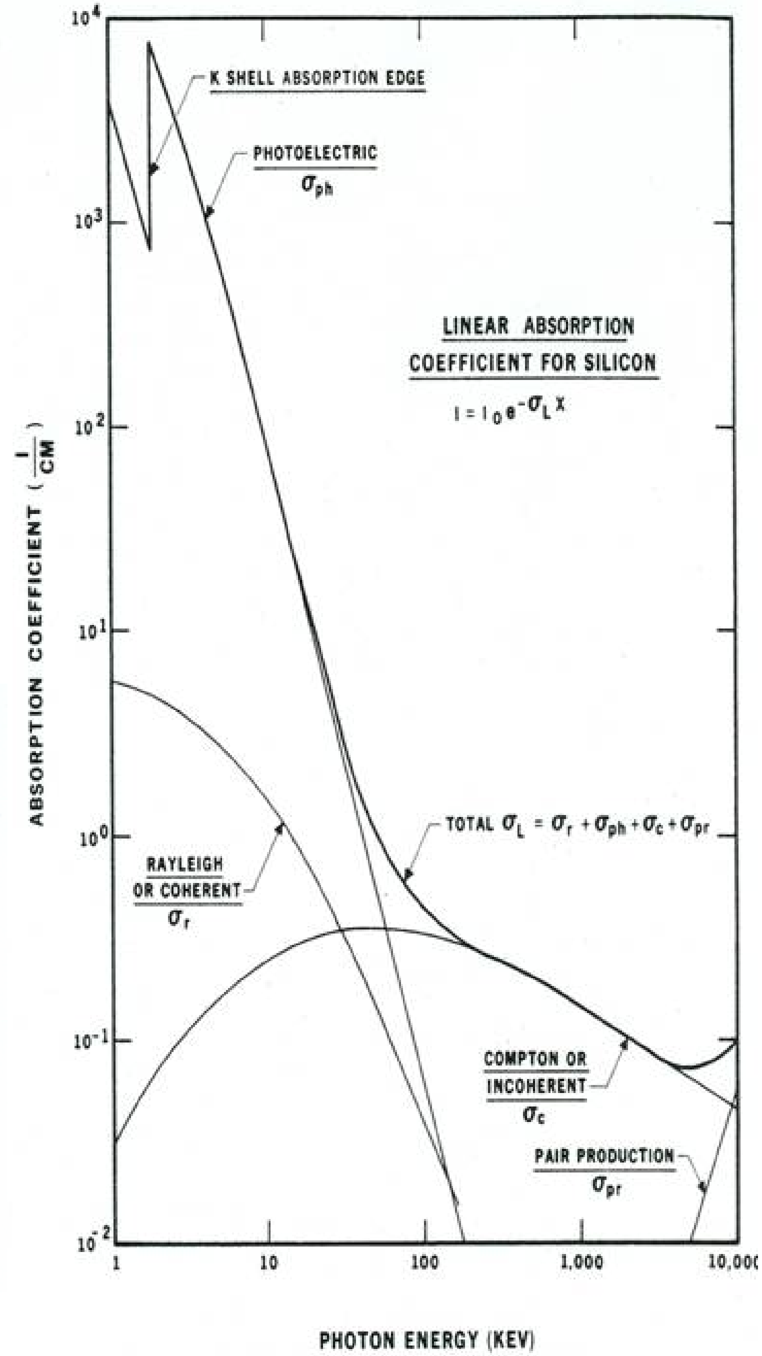

K SHELL ABSORPTION EDGE
PHOTOELECTRIC
σ_{ph}
LINEAR ABSORPTION
COEFFICIENT FOR SILICON
$I = I_0 e^{-\sigma_L x}$
TOTAL $\sigma_L = \sigma_r + \sigma_{ph} + \sigma_c + \sigma_{pr}$
RAYLEIGH
OR COHERENT
σ_r
COMPTON OR
INCOHERENT
σ_c
PAIR PRODUCTION
σ_{pr}
ABSORPTION COEFFICIENT ($\frac{1}{CM}$)
PHOTON ENERGY (KEV)

$$\sigma_{Si}{}^2 = F \cdot E_{photon} w$$

$$ENC_{par}{}^2 = qI_{leak} \int_{-\infty}^{\infty} h(t)^2 dt \approx qI_{leak} t_{peak}$$

$$ENC_{series}^2 = \tfrac{1}{2} e_n^2 C_t^2 \int_{-\infty}^{\infty} \left[h^{'}(t)\right]^2 dt \approx e_n^2 C_t^2 / t_{peak}$$

$$t_{peak}^{(optimal)} = e_n C_t / \sqrt{q \cdot I_{leak}}$$

$$w = 3.62eV$$

Leakage Current: $i_{leak} = q \cdot n_i / (2 \cdot \tau)$

Where n_i is the density of carrier in intrinsic silicon, tau is the life time and N_t the density of traps in silicon bulk.

$$n_i \propto \exp(-E_{gap} / (2kT))$$

$$\tau \cong 1/(\sigma \cdot v_{th} \cdot N_t)$$

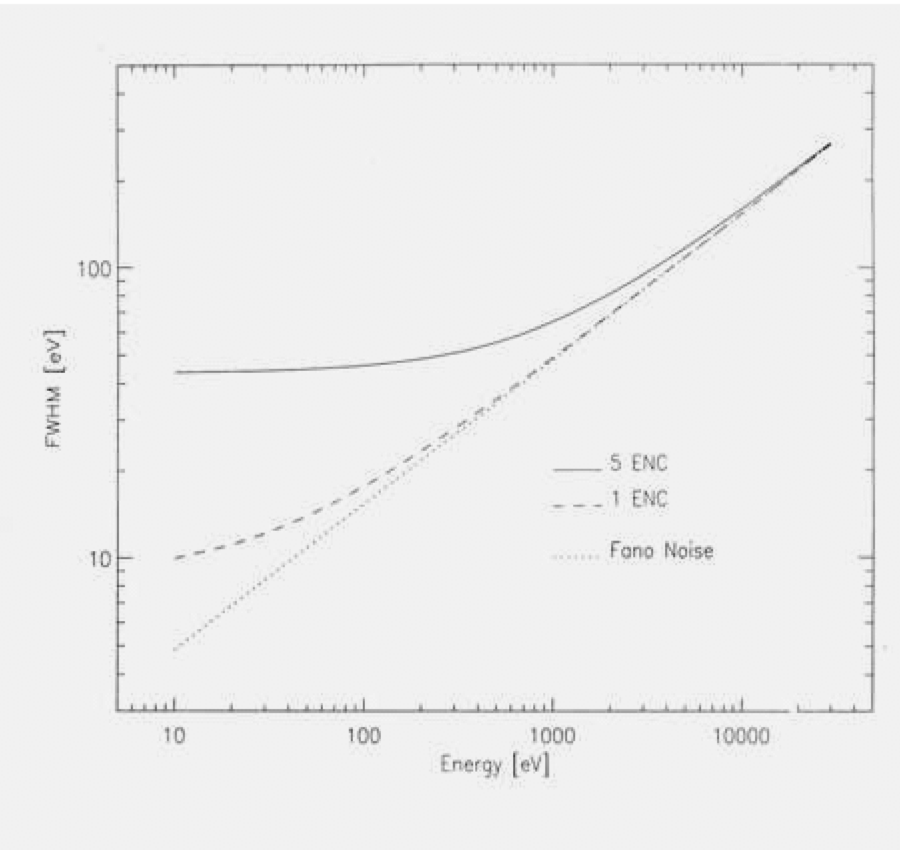

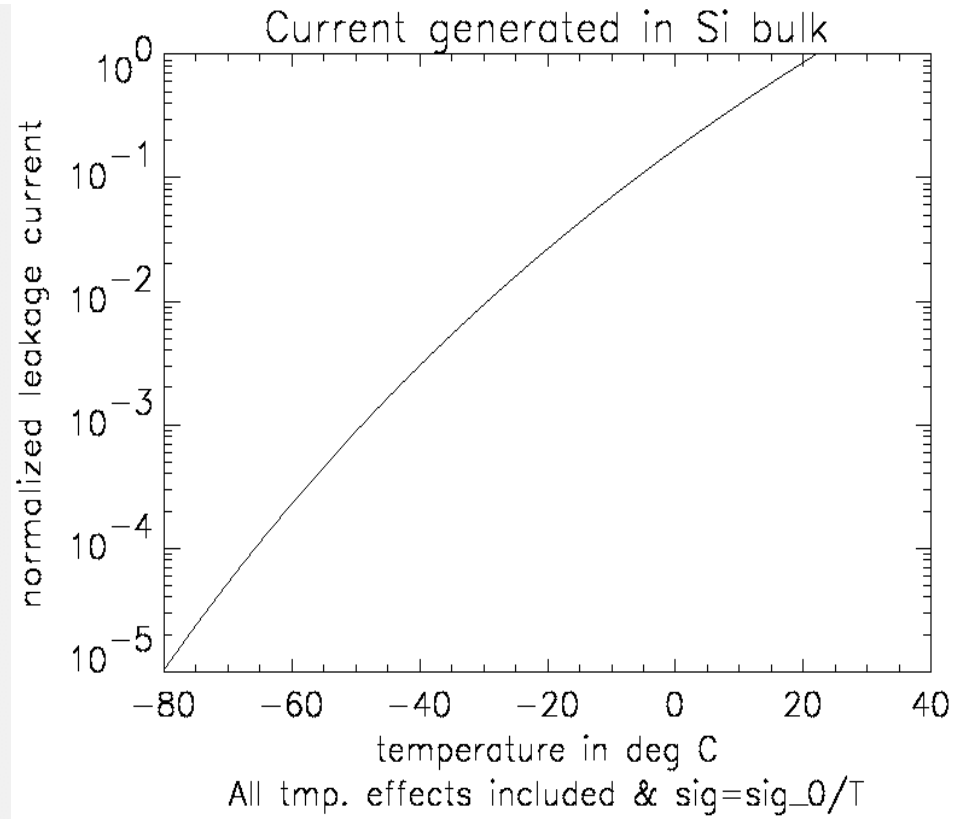

X-ray drift detector

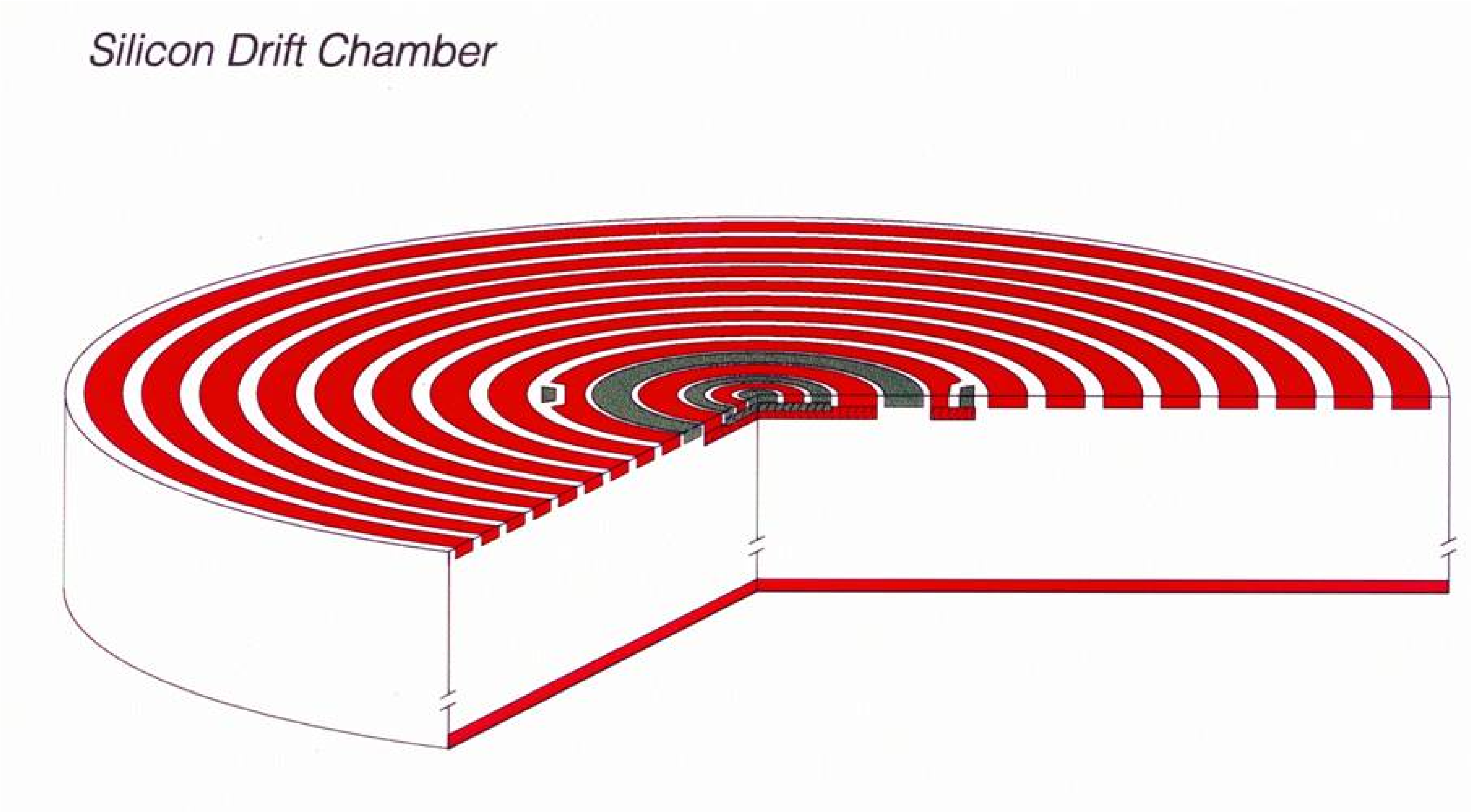

Potential within Drift Detectors

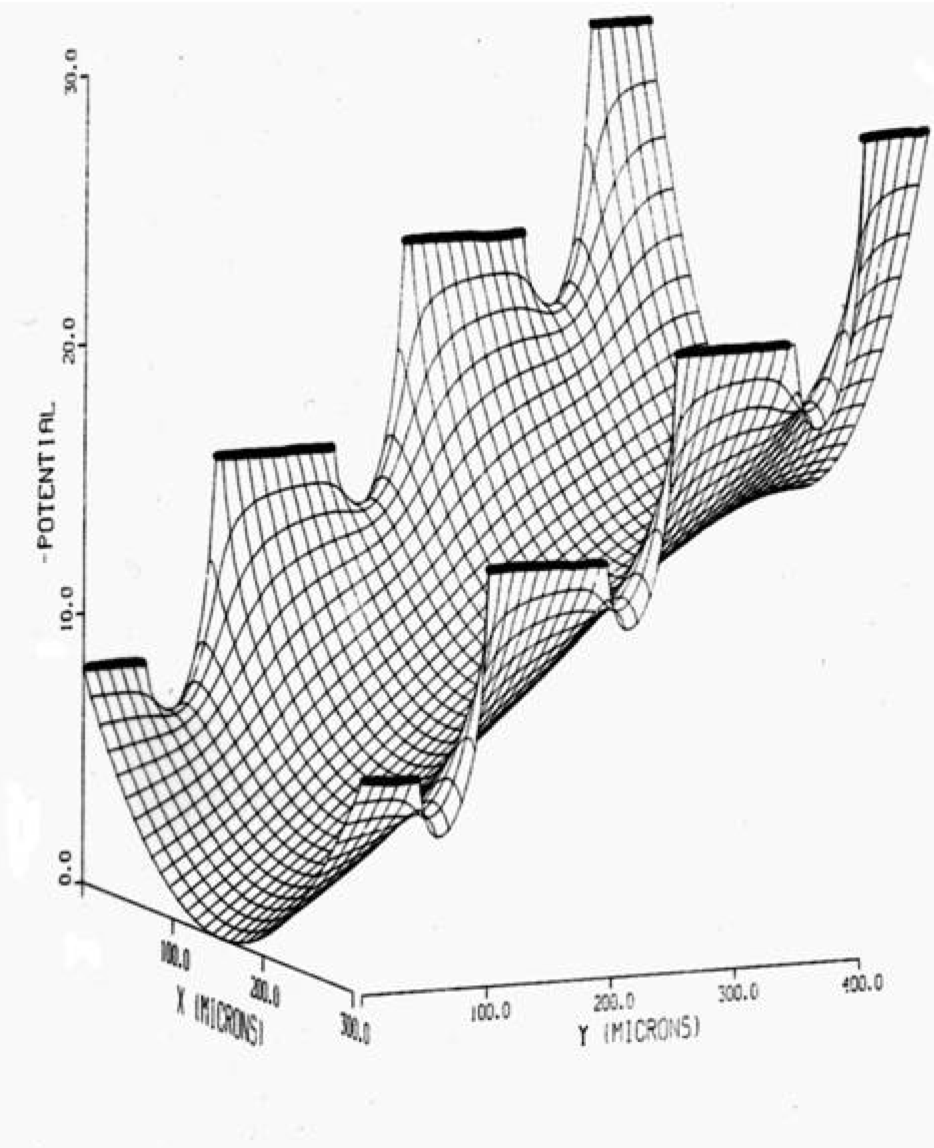

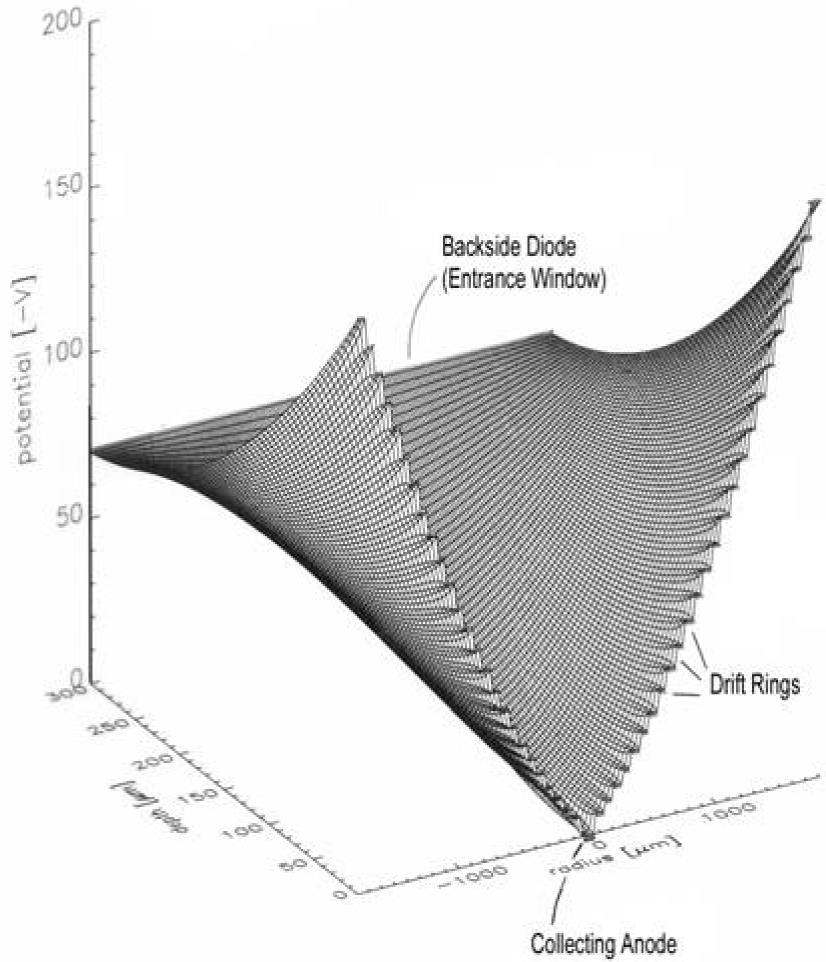

Single sided junction FET

N-Channel JFET on Depleted N-type Silicon

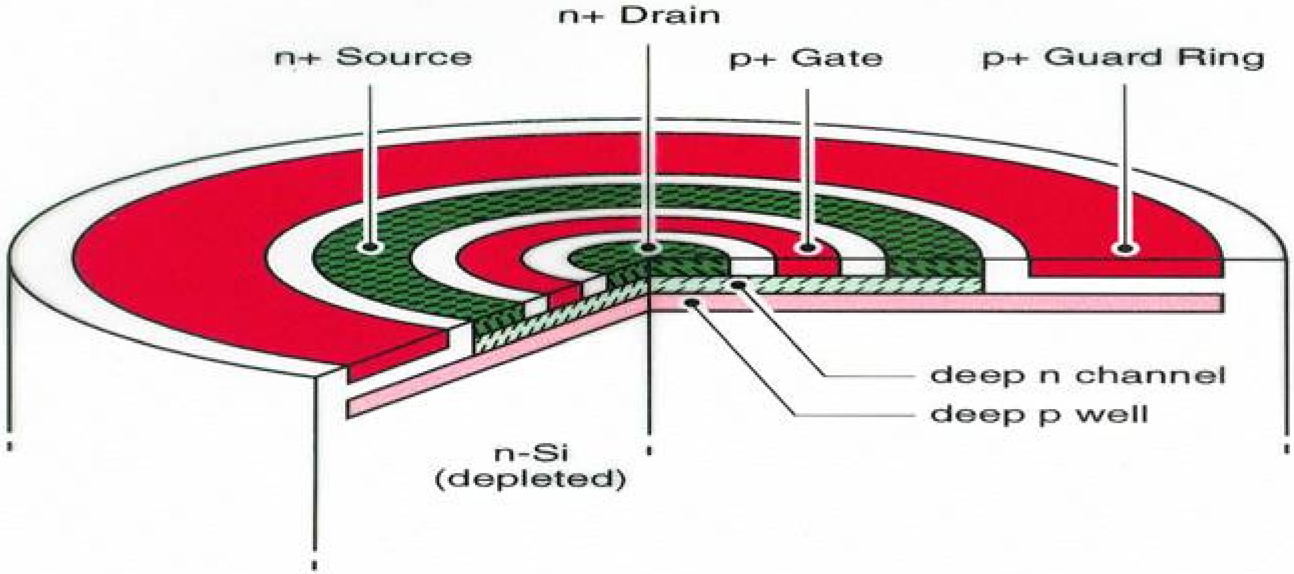

size & characteristics (typical):

gate length	5	µm
gate width	50	µm
saturation current	400	µA
transconductance	400	µA/V

The best room temp. spectrum

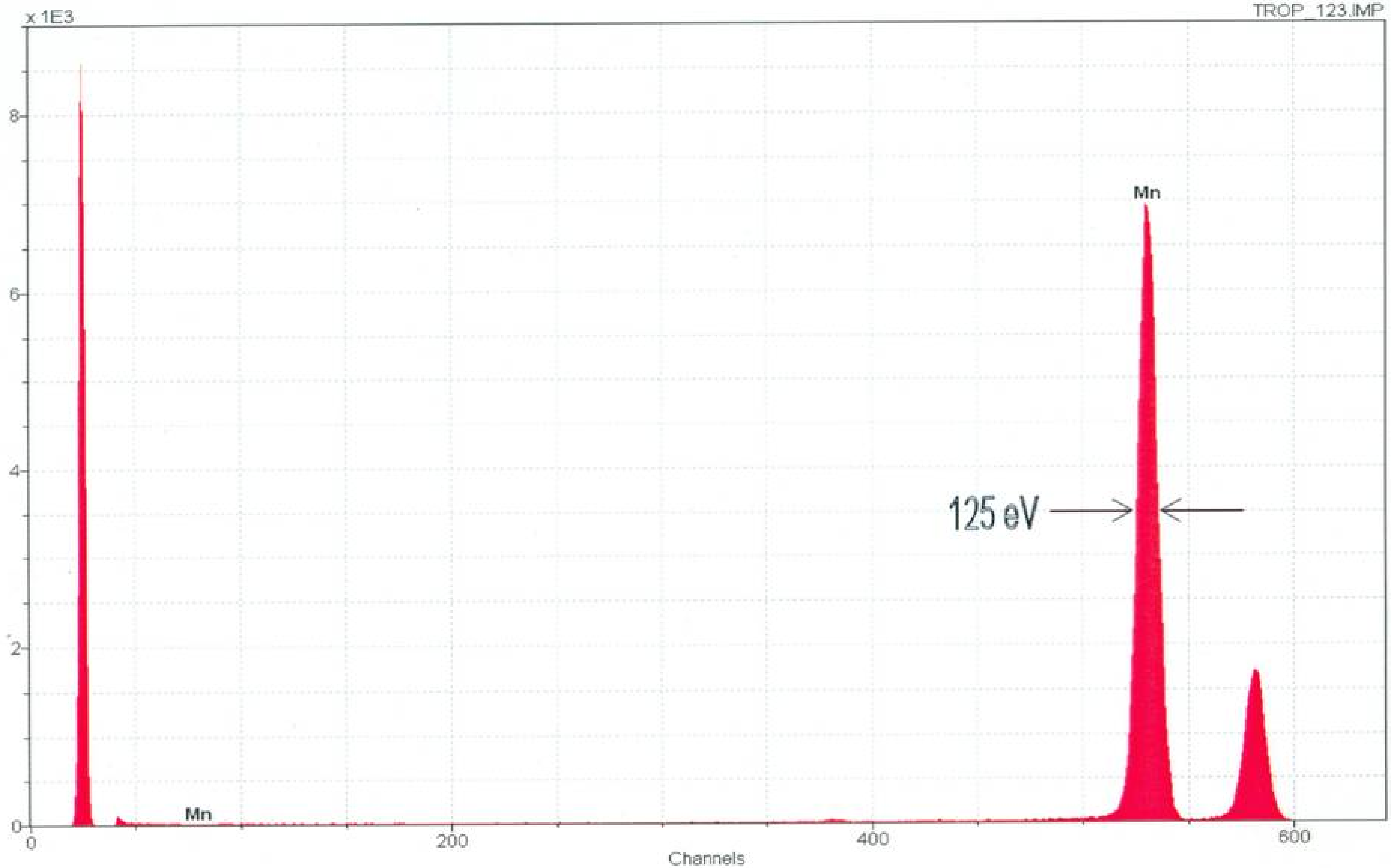

Low energy tails

Spectral Response

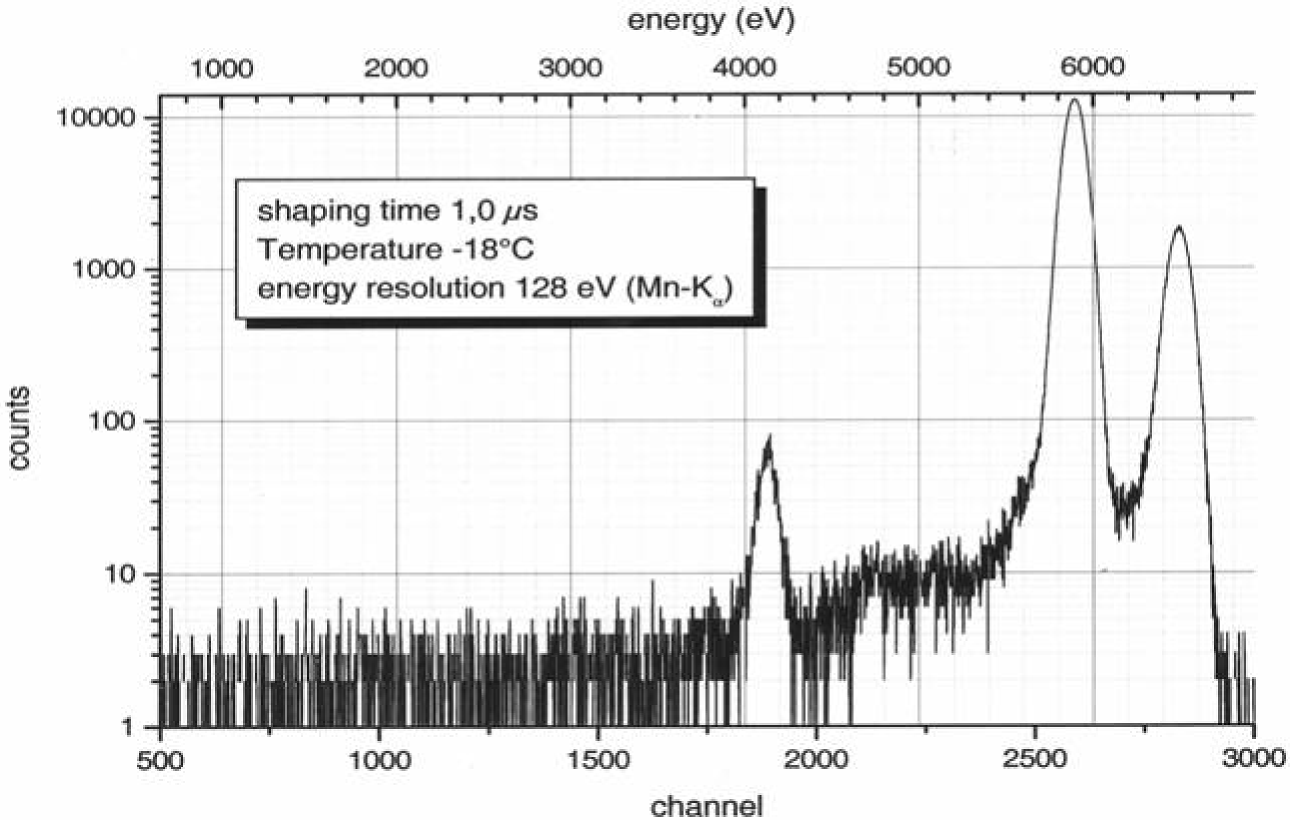

X-ray fluorescence system

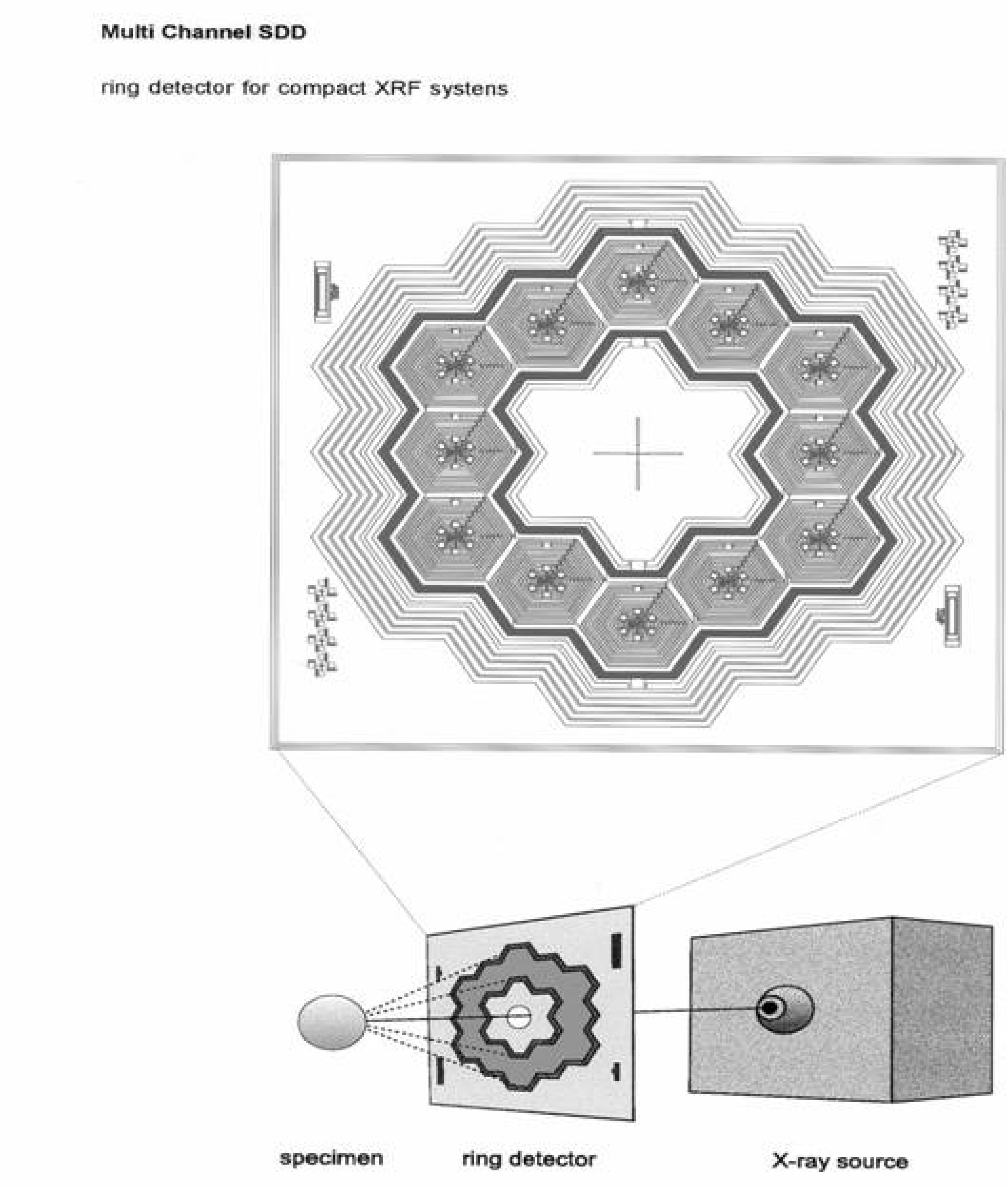

Applications in Art studies

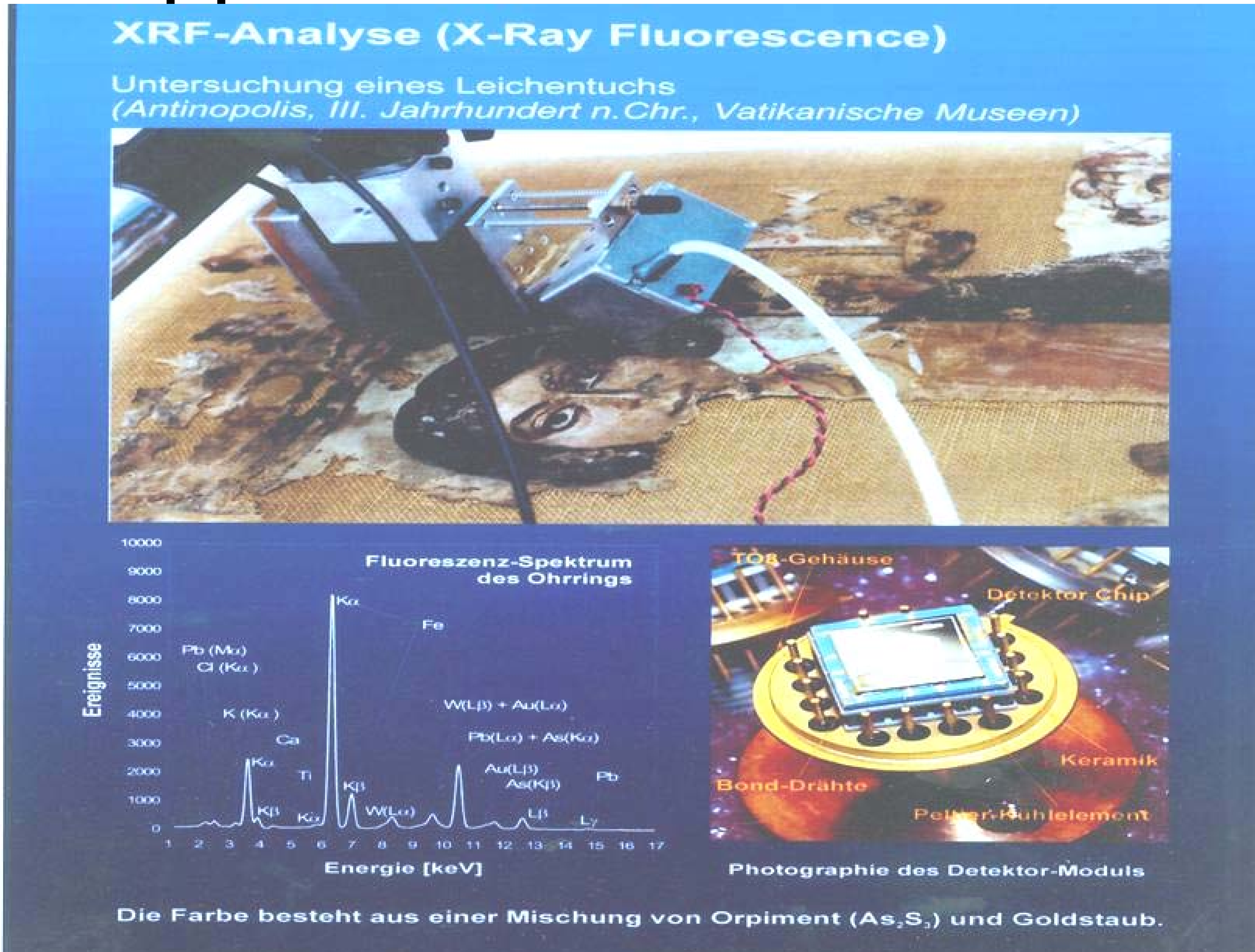

The *Controlled-Drift Detector* (CDD)*

(*) Patents:
US 6,249,033
EP0862226

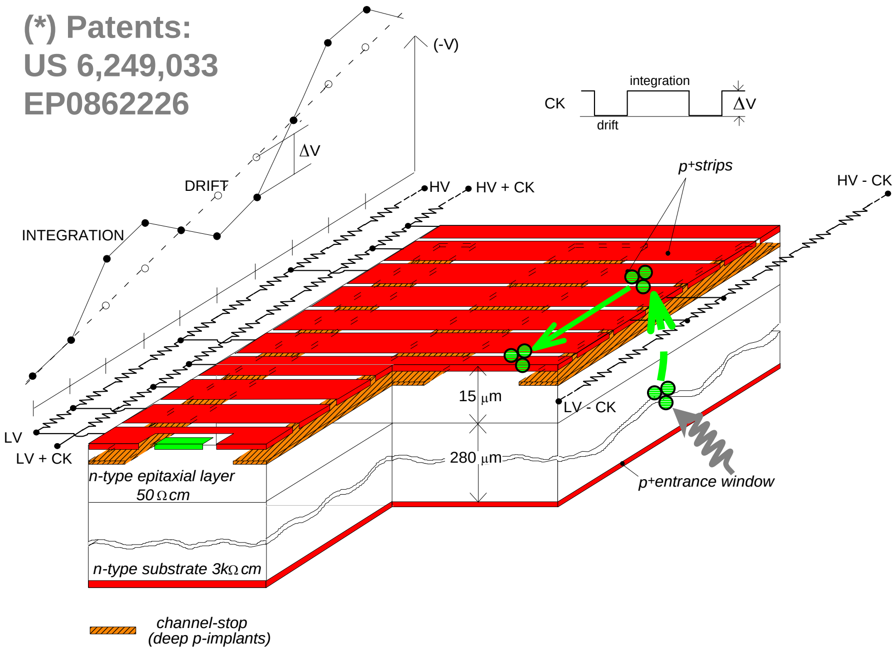

- 2D position sensing (100-200μm)
- low capacitance (~100fF) and integrated JFET ⇒ high energy resolution
- low no. of channels (n instead of $n \times n$)
- integrate-readout mode

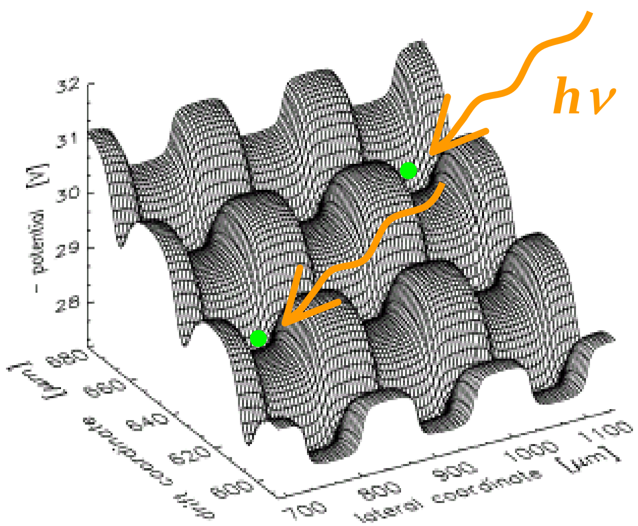

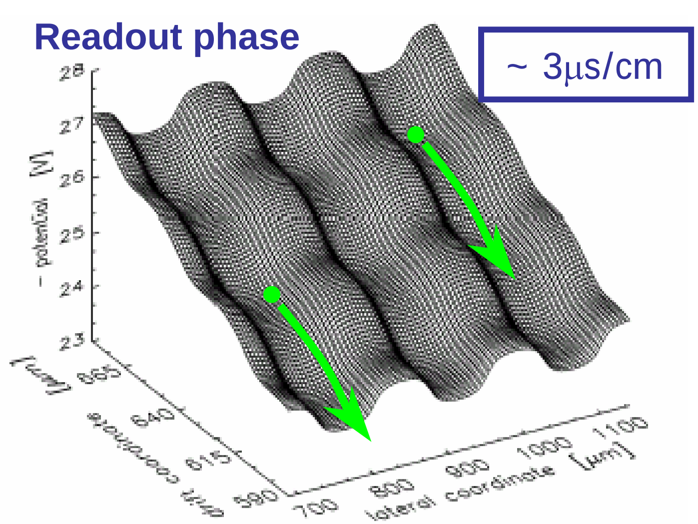

The <u>X-ray position</u> along the drift is obtained from the <u>electrons' drift time</u>

The <u>X-ray energy</u> is obtained from the <u>electron charge</u> collected at the anodes

Transport mechanism and Readout speed

Charge-Coupled Device (CCD)

L.Strüder et al., NIM A257 (1987) 594

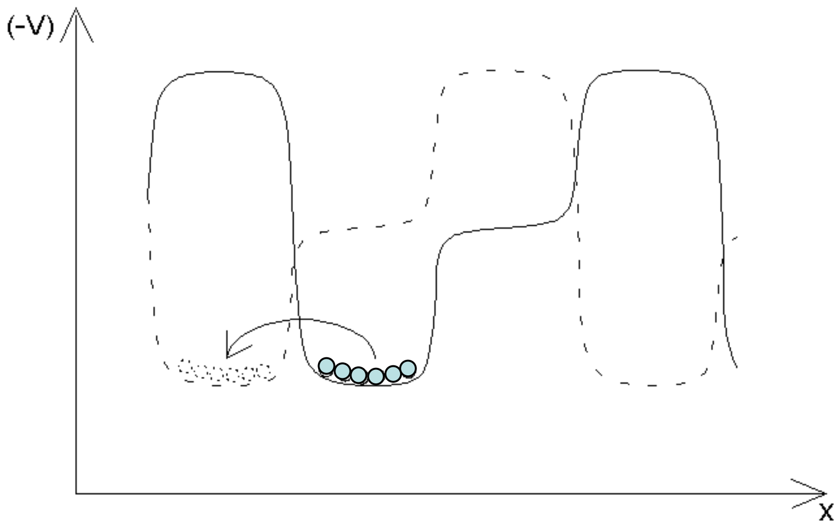

☹ **long readout time** as charge transfer and processing are done sequentially

$$T_{readout} = N_{pixel} \, (T_{proc} + \Delta t_{tr})$$

~ 1 ms/cm

Controlled Drift Detector

A.Castoldi et al., IEEE TNS, 44(5) oct. 1997 p.1724

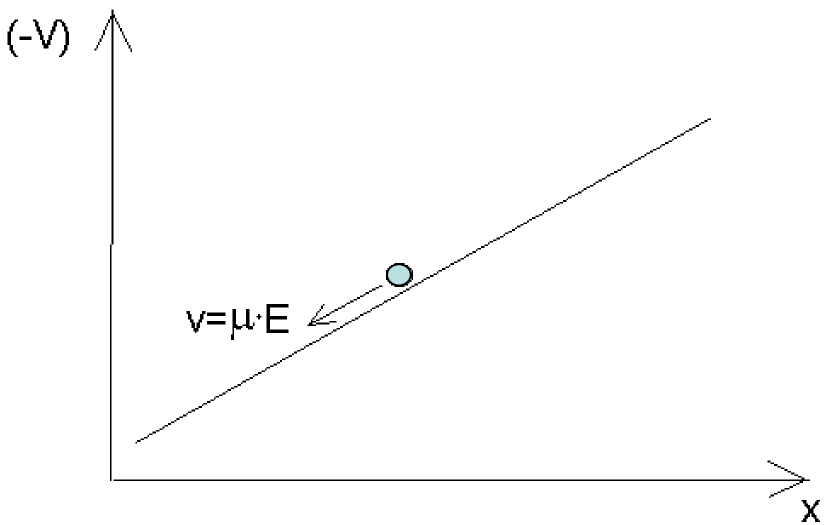

☹ **shorter readout time** as charge transfer and processing are simultaneous

$$T_{readout} = T_{drift}$$

~ 3 μs/cm

1-D imaging and spectroscopy of a Fe-55 source @ 100 kHz

A.Castoldi, C.Guazzoni, P.Rehak, L.Strüder, Trans. Nucl. Sci. 49 (3) June 2002

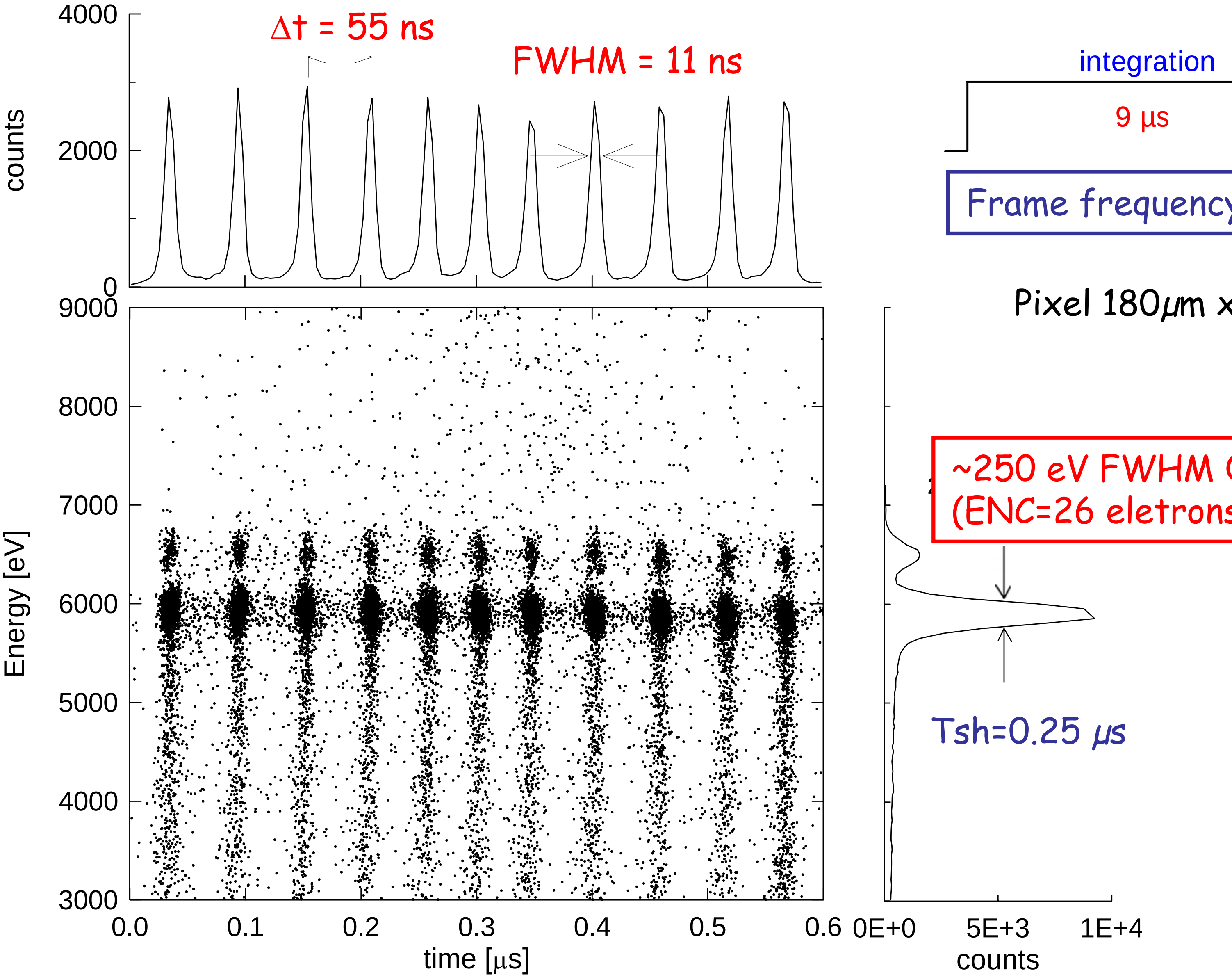

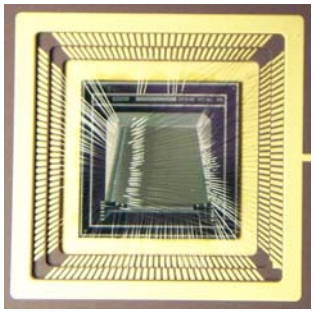

6x6 mm^2 prototype

X-ray spectroscopic imaging with CDDs

Radiographic image of a lizard*...

pixel 120μm, 10^5 frame/s, T=300 K

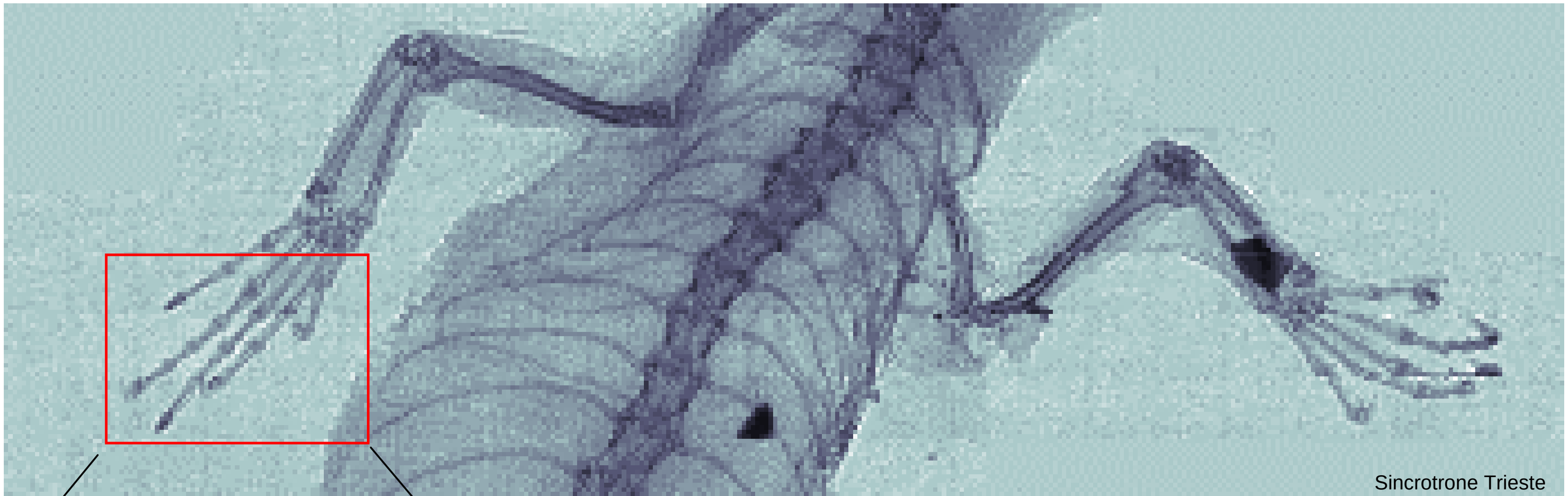

* no animal was killed ot has suffered for this measurement

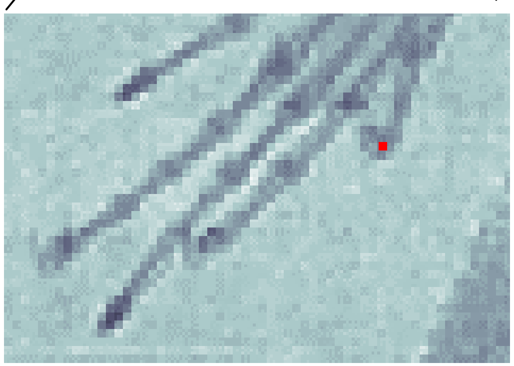

...and spectroscopic analysis of each pixel

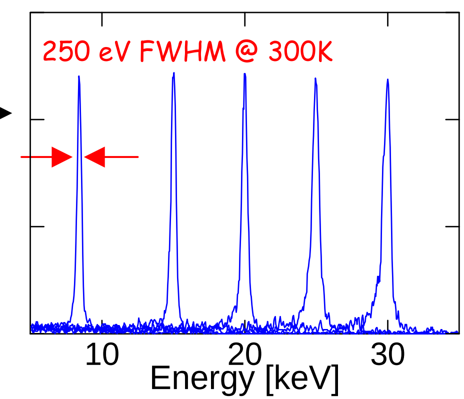

Readout speed and Energy resolution

A fast readout speed allows to reduce both readout and integration times:

⇓

- higher frame rate (i.e. better time resolution between X-ray images)
- better energy resolution at room temperature due to lower integrated leakage charge.

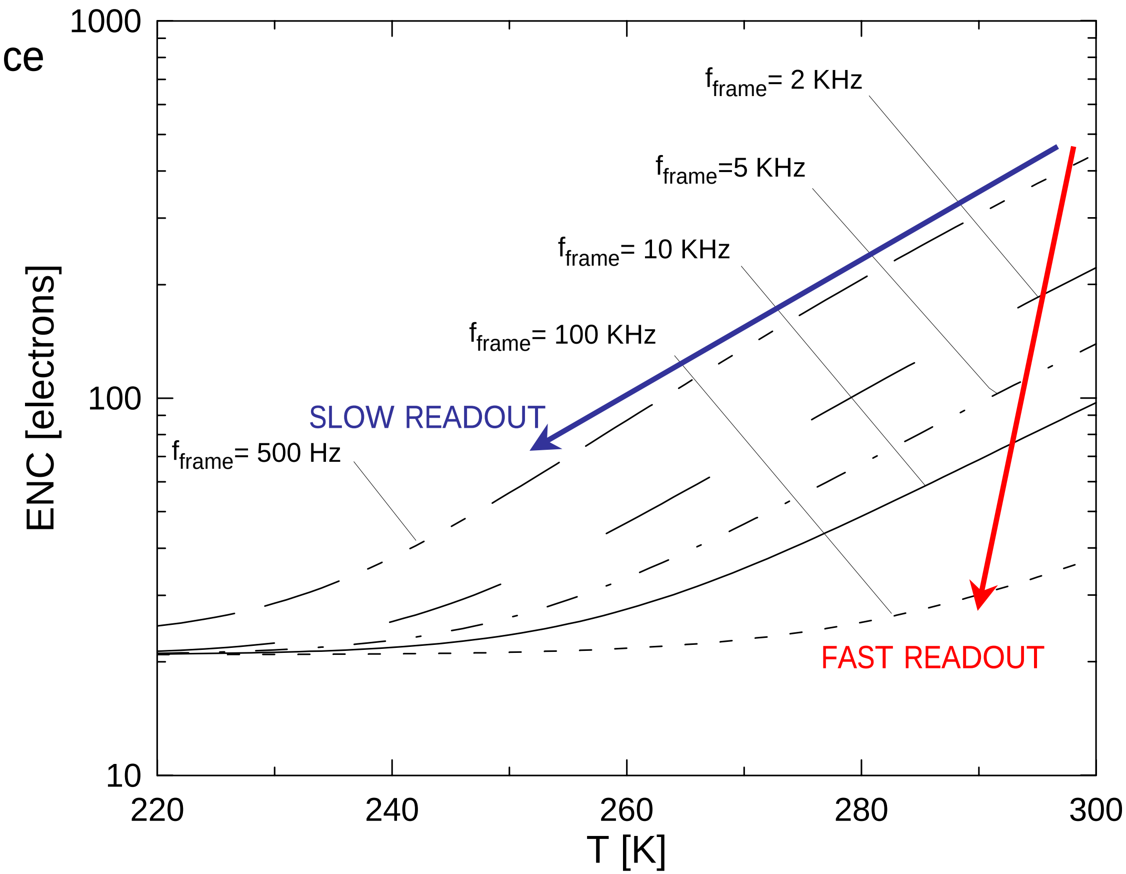

Time-resolved imaging at frame frequency greater than 10 kHz
State-of-the-art energy resolution near room T

Summary and Conclusions

- Extended use of SDD for tracking in high energy heavy ions experiments
- Industrial use of Silicon Drift Detectors for X-ray fluoroscopy
- Development of Controlled Drift Detector
- Use of Drift concept for Detectors on High Z materials. (insensitive to hole trapping)
- Future-high resistivity silicon for X-rays
- Future – tracking with electronics grade Si